# Automatic Interpretation of Schlumberger Sounding Curves, Using Modified Dar Zarrouk Functions

GEOLOGICAL SURVEY BULLETIN 1313-E

# Automatic Interpretation of Schlumberger Sounding Curves, Using Modified Dar Zarrouk Functions

*By* ADEL A. R. ZOHDY

NEW TECHNIQUES IN DIRECT-CURRENT RESISTIVITY EXPLORATION

GEOLOGICAL SURVEY BULLETIN 1313-E

*Formulas defining two types of modified Dar Zarrouk curves are used to invert Schlumberger sounding curves, using an iterative procedure. The number of layers, which is equal to the number of points on the inverted curve, is reduced by automatically smoothing the corresponding DZ curve*

UNITED STATES GOVERNMENT PRINTING OFFICE, WASHINGTON : 1975

UNITED STATES DEPARTMENT OF THE INTERIOR

JAMES G. WATT, *Secretary*

GEOLOGICAL SURVEY

Dallas L. Peck, *Director*

First printing 1975
Second printing 1983

For sale by the Distribution Branch, U.S. Geological Survey,
604 South Pickett Street, Alexandria, VA 22304

# CONTENTS



# ILLUSTRATIONS

NEW TECHNIQUES IN DIRECT-CURRENT RESISTIVITY EXPLORATION

# AUTOMATIC INTERPRETATION OF SCHLUMBERGER SOUNDING CURVES, USING MODIFIED DAR ZARROUK FUNCTIONS

By ADEL A. R. ZOHDY

ABSTRACT

For horizontally stratified media, Schlumberger VES (vertical electrical sounding) curves with slopes of greater than $-1$ not only resemble but commonly almost coincide with their corresponding DZ (Dar Zarrouk) curves. By considering an $n$-point Schlumberger VES curve to be an $n$-layer DZ curve, and by solving for the layering from the DZ curve, we obtain a first approximation to the actual layering in the form of an $n$-layer section. However, the minimum slope for DZ curves is $-1$, whereas on some VES curves negative slopes may be as low as $-3$; therefore, these VES curves cannot be considered to be a first approximation to their corresponding DZ curves. Formulas are obtained for calculating two types of MDZ (modified DZ) curves whose positive and negative slopes are not limited to $+1$ and $-1$, respectively. Therefore, for any VES curve, there exists a corresponding MDZ curve that lies close to it. The automatic interpretation is made by an iterative procedure in which, for the first approximation, the observed VES curve is assumed to be the sought MDZ curve. This MDZ curve is solved for layer thicknesses and resistivities; then, by means of a convolution technique, a VES curve is calculated for the obtained layering, and the calculated VES curve is compared with the observed one. A second approximation to the sought MDZ curve is obtained by utilizing the differences between the observed and calculated VES curves. The iteration is continued until a match, within a prescribed fitting tolerance, is obtained between observed and calculated VES curves. The number of layers in the resulting model (detailed solution) is always equal to the number of points used to define the observed VES curve. Equivalent solutions composed of a fewer number of layers are determined by automatically smoothing the DZ curve of the detailed solution and inverting it. Special equivalent solutions that are subject to certain geologic or geoelectric constraints can be found by manual adjustments of the detailed $n$-layer DZ curve. Excellent automatic matches were obtained when the method was tested with several theoretical VES curves and with several hundreds of field VES curves of different forms. The average processing time per VES curve (extending over more than three logarithmic cycles) on the IBM 360/65 computer is about 8 seconds. For distorted and incomplete field curves, the average processing time is approximately doubled.

## INTRODUCTION

The interpretation of VES (vertical electrical sounding) curves is usually made by curve-matching procedures in which albums of theoretical curves (Compagnie Générale de Géophysique, 1963; Flathe, 1963; Orellana and Mooney, 1966; Rijkwaterstaat, 1969) are used in conjunction with the auxiliary-point method of partial curve matching (Kalenov, 1957; Orellana and Mooney, 1966; Zohdy, 1965). Although this method is very educational and significant, it requires a great deal of practice, and at times it can be frustrating to the inexperienced interpreter. In fact, for geoelectric sections containing layers with small effective-relative resistances or small effective-relative conductances (Flathe, 1963; Zohdy and Jackson, 1973; Zohdy, 1974a), even the experienced interpreter may find it difficult to obtain satisfactory curve matches when he uses the auxiliary-point method. The use of DZ (Dar Zarrouk) curves (Maillet, 1947; Orellana, 1963) is valuable in improving the theoretical fit to an observed VES curve (Zohdy, 1974a), especially when the interpretation must be modified so that the interpreted geoelectric section would contain a different number of layers than the one initially assumed.

The direct interpretation, or inversion, of VES curves into layer thicknesses and resistivities has attracted the attention of geophysicists for the past 40 years. In late November 1972 the author presented a paper on automatic interpretation of Schlumberger sounding curves, using modified Dar Zarrouk functions, at the 42d annual international meeting of the Society of Exploration Geophysicists in Los Angeles, Calif. The present report is based on that talk and describes a fast method for the automatic interpretation of Schlumberger-type VES curves which are obtained over horizontally stratified, laterally homogeneous media. The method is intended for the processing of large numbers of VES curves on a digital computer in very short periods of time so that the interpreter may have at his disposal a basic solution, and simplified solutions, for each observed VES curve. The basic solution also may be modified manually, through the use of DZ curves, to obtain electrically equivalent solutions that will fit certain constraints on the layering in the survey area. The layering provided by the computer, moreover, may be considered as an interpretation made by an independent interpreter whose computations do fit the observed data and, therefore, often may point out a certain layering distribution which the interpreter may have overlooked.

The method was designed so that positive, realistic, layer resistivities and thicknesses are always obtained, even if the VES curve is distorted by lateral heterogeneities. For these distorted VES curves, although a practically perfect match between observed and calculated curves may be impossible (because the solution is based on a horizontally stratified,

laterally homogeneous earth model), the calculated curve will fit the observed points as closely as possible, except for those points near the distorted segment.

## EARLIER DEVELOPMENTS

Several methods have been proposed for the direct interpretation, or inversion of VES curves obtained over horizontally stratified, laterally homogenous media. Stefanesco and others (1930) derived the integral expressions

$$V(r)=\frac{\rho_1 I}{2\pi}\left[\frac{1}{r}+2\int_0^\infty \Theta(\lambda,k,d)J_0(\lambda r)d\lambda\right] \tag{1}$$

$$\bar{\rho}_s(r)=\rho_1\left[1+2r^2\int_0^\infty \Theta(\lambda,k,d)J_1(\lambda r)\lambda\, d\lambda\right] \tag{2}$$

for expressing the potential $V(r)$ and the Schlumberger apparent resistivity $\bar{\rho}_s(r)$ as a function of the Schlumberger electrode spacing, $r=AB/2$; the first-layer resistivity, $\rho_1$; the Bessel functions, $J_0$ and $J_1$; and the Stefanesco kernel function, $\Theta(\lambda,k,d)$, which is expressed in terms of the layer depths, $d$; the resistivity reflection coefficients, $k$, and the integration variable, $\lambda$. If the TKF (total kernel function), $T(\lambda,d,k)$, also known as the Schlichter kernel (Vozoff, 1958), is defined by

$$T(\lambda,d,k)=\rho_1[1+2\Theta(\lambda,d,k)]; \tag{3}$$

then,

$$\Theta(\lambda,d,k)=[(T(\lambda,d,k)/\rho_1)-1]/2. \tag{4}$$

Substituting equation 4 in equation 1 we get

$$V(r)=\frac{\rho_1 I}{2\pi}\left[\frac{1}{r}+\int_0^\infty \frac{T(\lambda,d,k)}{\rho_1}J_0(\lambda r)\mathrm{d}\lambda-\int_0^\infty J_0(\lambda r)d\lambda\right]. \tag{5}$$

But, according to the Weber-Lipschitz identity (Watson, 1962),

$$\frac{1}{r}=\int_0^\infty J_0(\lambda r)d\lambda, \tag{6}$$

and therefore (Sunde, 1949) equation 5 reduces to

$$V(r)=\frac{I}{2\pi}\int_0^\infty T(\lambda,d,k)J_0(\lambda r)d\lambda. \tag{7}$$

Differentiating equation 7 with respect to $r$ and substituting in the equation

$$\bar{\rho}_s(r) = -\frac{2\pi}{I} r^2 \frac{dV}{dr}, \tag{8}$$

we get

$$\bar{\rho}_s(r) = r^2 \int_0^\infty T(\lambda,d,k) \cdot J_1(\lambda r) \cdot \lambda d\lambda. \tag{9}$$

With an appropriate change in the variables $r$ and $\lambda$, the integral in equation 9 can be transformed into a convolution integral (Kunetz, 1966).

Inasmuch as the kernel function, $T$ or $\Theta$, contains all the information that is necessary to define the geoelectric section (layer thicknesses and resistivities), Schlichter (1933) suggested the following procedure for the direct interpretation of resistivity sounding data:

1. Determine the kernel-function curve from the apparent resistivity curve,
2. Solve for the layering from the kernel function.

The value of $T(\lambda,d,k)$ can be expressed in terms of the Schlumberger apparent resistivity by applying the inverse Hankel transformation of the Fourier-Bessel integral (Watson, 1962) to equation 9 so that

$$T(\lambda,d,k) = \int_0^\infty \bar{\rho}_s(r) \frac{J_1(\lambda r)}{r} dr. \tag{10}$$

The numerical evaluation of $T(\lambda,d,k)$ from equation 10 has been studied by several investigators. Strakhov (1966a, 1966b, 1968) derived expressions for the calculation of $T(\lambda,d,k)$, and Strakhov and Karelina (1969) published coefficients for the transformation of a Schlumberger VES curve into its corresponding TKF curve, using convolution. In order to make this transformation, using the Strakhov-Karelina coefficients, the VES curve must be digitized at the logarithmic electrode-spacing interval of $(AB/2)_{i+1}/(AB/2)_i = e^{(\ln\ 10/5)} \simeq 1.58$, which is equivalent to five logarithmically equally spaced points per logarithmic cycle. The digitized apparent resistivities are convolved with the Strakhov-Karelina coefficients to obtain the total-kernel-function curve.

Ghosh (1971a) used linear-filter theory to obtain other sets of coefficients for transforming Schlumberger and Wenner sounding curves into their corresponding TKF curves. Ghosh's coefficients are applicable for the logarithmic electrode-spacing interval of of $(AB/2)_{i+1}/(AB/2)_i = e^{(\ln\ 10/3)} \simeq 2.15$, but, for a greater definition of the calculated TKF curve, his coefficients may be convolved with

two sets of digitized points on the VES curve, which are separated by an interval of 1.46, to obtain points on the TKF curve which are separated by a factor 1.46 instead of 2.15.

The use of convolution for the calculation of the TKF curve from an observed VES curve requires the extrapolation of the VES curve to the left of the first and to the right of the last measured points. The values of the ordinates of the extrapolated VES points not only will affect the values of the calculated TKF curve at the TKF points corresponding to the first and last VES points but also will affect the values of several successive TKF points to the right and to the left of the first and last calculated points, respectively. Furthermore, a distortion over a small segment of the VES curve will cause a distortion over a correspondingly larger segment on the transformed TKF curve.

Koefoed (1965, 1966, 1968) used the raised kernel function $H(\lambda)$ instead of the Stefanesco kernel function $\Theta(\lambda)$ and subsequently (Koefoed, 1970) introduced graphs to accelerate the evaluation of the layer thicknesses and resistivities from the raised kernel function $H(\lambda)$. Other students of the direct interpretation of resistivity data in the kernel domain include Crous (1971), Meinardus (1967, 1970), Onodera (1960), Pekeris (1940), and Vozoff (1958).

One of the most attractive features of transforming a VES curve into its corresponding TKF curve (and finding the appropriate horizontally layered model for which a calculated TKF fits the transformed curve) is the ease with which a TKF curve can be calculated using Sunde's, Flathe's, or Vanyan's recursion formulas (Sunde, 1949; Flathe, 1955; Vanyan and others, 1962; Kunetz, 1966; Meinardus, 1967). Russian geophysicists have compiled albums of theoretical TKF curves and prepared equivalence nomograms similar to the Pylaev nomograms (Bhattacharya and Patra, 1968) for the interpretation of transformed TKF curves by the method of curve matching (Shkabarnia and Gritsenko, 1971).

Kunetz and Recroi (1970) pointed out some of the limitations of the interpretation of VES curves in the kernel domain, such as the risk of rapid amplification of errors in the initial data and the possibility, with certain techniques, of obtaining solutions that are physically absurd (for example, negative resistivities and (or) negative thicknesses). Furthermore, because the maximum negative slope for a TKF curve is $-1$, similar to DZ curves, the resolving power of TKF curves for Q-type ($\rho_1>\rho_2>\rho_3$) and certain HK-type ($\rho_1>\rho_2<\rho_3>\rho_4$) sections is lower than the resolving power of the corresponding VES curves; therefore, the range of the principle of equivalence, in the kernal domain, is larger than it is for VES curves (Strakhov and Karelina, 1969). In other words, if two TKF curves seem to coincide (where one curve was obtained by the transformation of an observed VES curve and the other was

calculated for an assumed model), it does not mean, necessarily, that their corresponding VES curves will also almost coincide. Therefore, for interpretations in the kernel domain, the calculation of the VES curve for comparison with the observed VES curve is advisable, especially for VES curves with steeply descending branches. In this regard, although Kunetz and Recroi based their analysis on the determination and solution of a "nucleus" kernel function, they were the first to show the applicability of their technique by comparing reference or observed VES curves with calculated VES curves, and not by comparing kernel function curves.

Kunetz (1966) indicated that it is possible to calculate VES curves by convolving the TKF curve with a set of coefficients which he did not publish. Ghosh (1971b) published two sets of inverse filter coefficients for the calculation of Schlumberger and Wenner VES curves by the method of convolution. The convolution technique is the fastest known method for the calculation of a VES curve. For example, a VES curve of the Schlumberger type, which is defined by 18 points that are distributed over three logarithmic cycles and which corresponds to a section composed of about 20 layers, can be calculated using the Ghosh coefficients in less than about 0.5 second on the IBM 360/65 computer (Zohdy, 1974b). With the advent of this technique, one of the most attractive features of interpreting VES curves in the kernel domain, namely the speed with which a TKF curve can be calculated, was rendered less significant.

The use of numerical integration (Meinardus, 1967, 1970) yields more accurate but slower (by several seconds) computations of VES curves than the use of convolution. The numerical integration method, however, is at least 10–20 times faster than the methods that are based on the summation of a slowly convergent series (Mooney and others, 1966). Furthermore, both the convolution method and the numerical integration method are not dependent on the condition that the layers in the section must be of commensurate thicknesses (thicknesses that are whole multiples of a given unit of length).

## OUTLINE OF METHOD

The automatic interpretation method presented here is based on inverting the VES curve without first transforming it into its corresponding TKF curve. Furthermore, unlike most of the direct interpretation methods, the interpreter does not have to make an initial assumption on the number of layers or about their resistivities and thicknesses. Instead, the VES curve is digitized (at the rate of six points per logarithmic cycle), and the number of layers is automatically fixed as equal to the number of points on the digitized curve.

For the first approximation, the points on the digitized VES curve are

considered to be points on a modified Dar Zarrouk (MDZ) curve, which is solved for layer thicknesses and resistivities. The TKF curve for this layering is calculated by Sunde's recursion formula, and the VES curve is calculated by convolution, using Ghosh's coefficients. The calculated and observed VES curves are compared, and, through an iterative formula, a new MDZ curve is calculated, solved for layering, and a second VES curve is calculated. The iteration continues until a fit, within a prescribed tolerance, is obtained between observed and calculated VES curves. In this procedure the calculation of the VES curve by convolution requires the calculation of the TKF curve at $(1/\lambda)$ values that extend beyond the range of the corresponding $(AB/2)$ values. However, because these TKF values are calculated for a given model by a recursion formula and are not calculated by the transformation of a VES curve, they are all accurately determined over the entire range of $(1/\lambda)$ values.

## CONSTRUCTION AND INVERSION OF DZ CURVES

DZ curves for $n$-layer sections are calculated from the parametric equations

$$\rho_{m_j}=\sqrt{\sum_1^j \rho_i h_i / \sum_1^j (h_i/\rho_i)}=\sqrt{\sum_1^j T_i / \sum_1^j S_i}\,, \tag{11}$$

and

$$L_{m_j}=\sqrt{\sum_1^j \rho_i h_i \cdot \sum_1^j (h_i/\rho_i)}=\sqrt{\sum_1^j T_i \cdot \sum_1^j S_i}\,, \tag{12}$$

where $\rho_{m_j}$ and $L_{m_j}$ are the DZ resistivity and DZ depth; $\rho_i$ and $h_i$ are the resistivity and thickness of the $i$th layer; and $T_i$ and $S_i$ are the transverse resistance and longitudinal conductance of the $i$th layer, respectively.

Figure 1 shows a set of two-layer DZ curves calculated for various values of $\mu=\rho_2/\rho_1$. It is important to note that the maximum positive and negative slopes for $\rho_2=\infty$ and $\rho_2=0$ are $+1$ and $-1$, respectively. Graphical methods were devised by Orellana (1963) and by Zohdy (1974a), for the construction of multilayer DZ curves.

The inversion of DZ curves into layer thicknesses and resistivities is made using the formulas

$$\rho_j=\sqrt{\frac{L_{m_j}\rho_{m_j}-L_{m_{j-1}}\rho_{m_{j-1}}}{\dfrac{L_{m_j}}{\rho_{m_j}}-\dfrac{L_{m_{j-1}}}{\rho_{m_{j-1}}}}}\,, \tag{13}$$

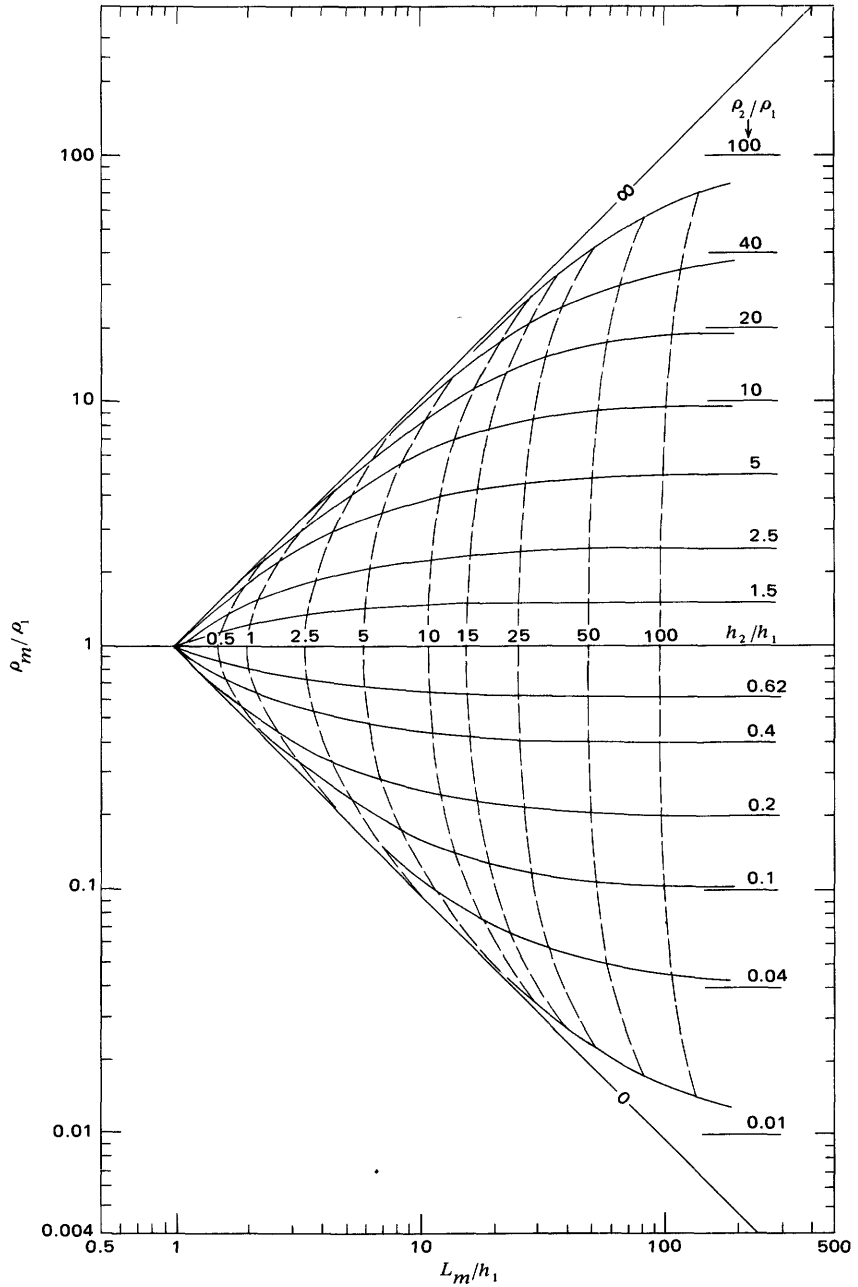


FIGURE 1. — Two-layer DZ curves for various values of the resistivity ratio $\rho_2/\rho_1$. Dashed curves designate the thickness ratio $h_2/h_1$. $\rho_m$, DZ resistivity; $L_m$, DZ depth; $\rho_1$ and $h_1$, first-layer resistivity and thickness.

$$h_j=\rho_j\left(L_{m_j}/\rho_{m_j}-L_{m_{j-1}}/\rho_{m_{j-1}}\right). \tag{14}$$

The above relationships are schematically summarized in figure 2; practical applications of the inversion of DZ curves (pertaining to the interpretation of VES curves) were given by Zohdy (1974a).

Figure 3 shows that Schlumberger VES curves on which there are no negative slopes of less than or equal to $-1$ commonly almost coincide with their corresponding DZ curves. If these DZ curves are solved for layering, using equations 13 and 14, either by using only the terminal DZ points (which mark the end of one layer and the beginning of another) or by digitizing the DZ curves so that the terminal points are included, we obtain the exact geoelectric sections for which both the DZ and VES curves were calculated. Therefore, because of the near coincidence of these VES curves with their corresponding DZ curves, a first approximation of the actual layering can be obtained by digitizing the VES curves, and substituting, in the inversion equations 13 and 14, the

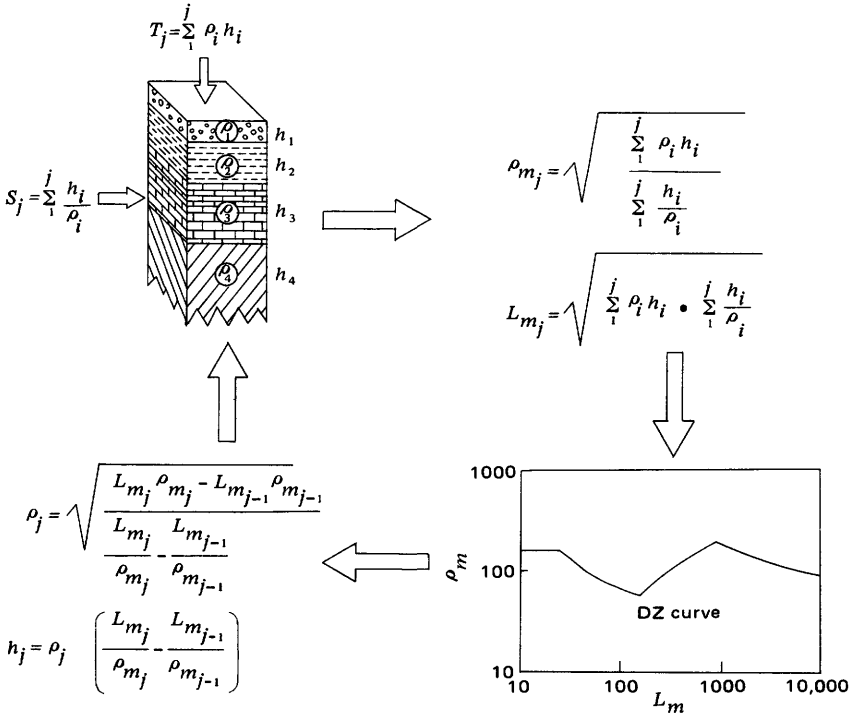


FIGURE 2. — Schematic diagram of the construction and inversion of DZ curves. $h_j$, layer thickness; $\rho_j$, layer resistivity; $T$, transverse resistance; $S$, longitudinal conductance; $\rho_m$, $DZ$ resistivity; $L_m$, DZ depth.

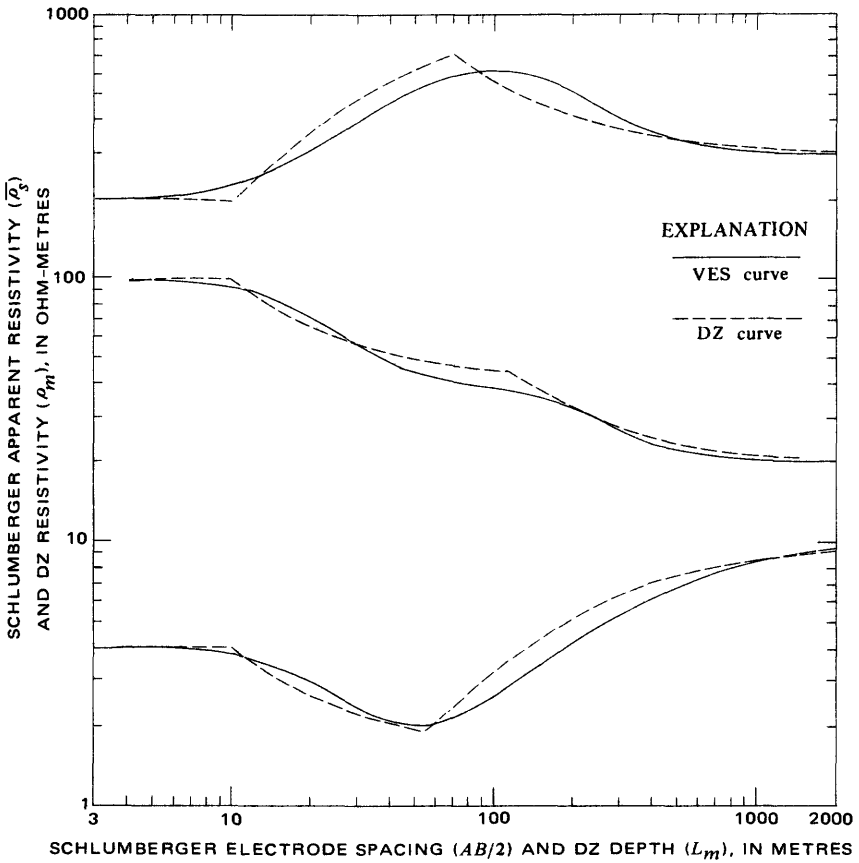


FIGURE 3. — Graphs of theoretical Schlumberger VES curves and their corresponding DZ curves.

values of the electrode spacings, $AB/2$, for the DZ depths, $L_m$, and the Schlumberger apparent resistivities, $\rho_s$, for the DZ resistivities, $\rho_m$, respectively.

Figure 4 shows five steps for the successive approximation of a layering for a theoretical VES curve. Step 1 shows the layering, the VES curve, and the DZ curve for an A-type section ($\rho_1<\rho_2<\rho_3$). By digitizing the VES curve, as shown in step 2, assuming that the VES curve is a DZ curve, and solving for the layering, we obtain the $n$-layer section shown by the dashed line. This layering serves as a first approximation to the true layering. By calculating the TKF curve for the $n$-layer section from Sunde's recursion formula and convolving it with Ghosh's coefficients, the VES curve for this layering can be calculated and plotted as shown by the dashed curve of VES′ in step 3. By knowing the effect of changes

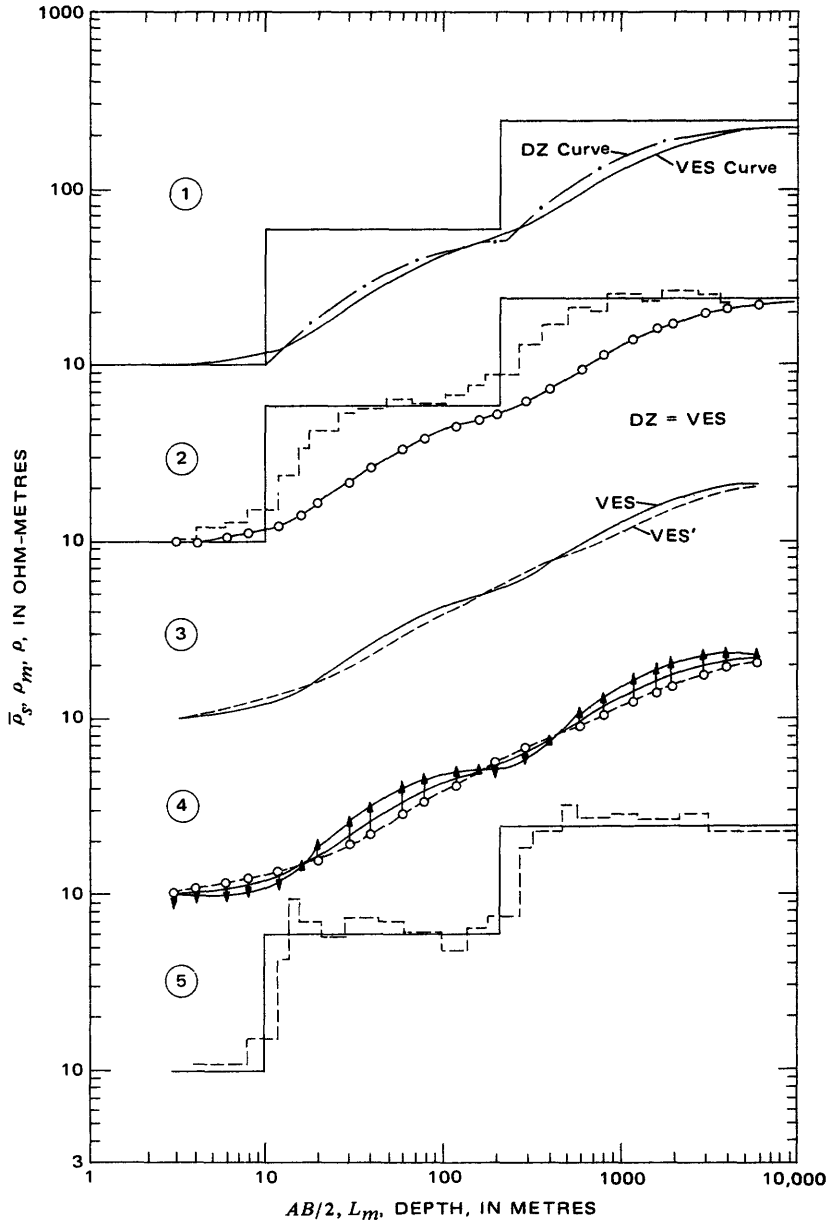


FIGURE 4. — Graphs showing the inversion of a three-layer VES curve of the A-type by iteration through successive approximations of its corresponding DZ curve. Circles on VES curve designate first approximation to DZ curve. Arrow heads designate second approximation to DZ curve.

in the form of DZ curves on the form of their corresponding VES curves, as they were recently described by Zohdy (1974a) we could have predicted the approximate shape of the VES′ curve in relation to the shape of the reference VES curve by noting the deviations of the ordinates of the reference VES curve from the ordinates of its corresponding DZ curve.

In order to obtain a second approximation to the layering, we obtain a second approximation to the actual DZ curve by utilizing the differences between the ordinates of the calculated (VES′) and reference VES curves. As shown in step 4, of figure 4, for points on the calculated VES′ curve that lie above the reference VES curve, we calculate new points (which are depicted by the arrow heads in step 4) which lie below the reference VES curve, and conversely. In step 5, the layering obtained from the inversion of this second approximation to the DZ curve is compared with the layering of the actual three-layer model. The calculation of the corresponding VES curve indicated that the two geoelectric sections are equivalent in the VES domain (that is, the two VES curves practically coincided). Had it been necessary to use several successive approximations to the DZ curve, the following iterative formula

$$\rho_{m_{i+1}} = \frac{\rho_{s_0} \cdot \rho_{m_i}}{\bar{\rho}_{s_i}} \tag{15}$$

would have been used where $\rho_{m_{i+1}}$=the $(i+1)$ DZ resistivity, $\bar{\rho}_{s_0}$=the ordinates of the reference VES curve, $\rho_{m_i}$=ordinates of the DZ resistivity for the $i$th iteration, and the $\bar{\rho}_{s_i}$=ordinate of the $i$th calculated VES curve.

To summarize, for the first approximation we use

$$\rho_m = \bar{\rho}_{s_0}, \tag{16}$$

for the second approximation, the iterative equation 15 reduces to

$$\rho_m = \frac{\bar{\rho}_{s_0}^{\,2}}{\bar{\rho}_{s_1}}, \tag{17}$$

and for the $(i+1)$ to the $n$th approximation we use equation 15.

The simplicity of the above procedure makes it very attractive for the automatic interpretation of VES curves; nevertheless, the procedure has two drawbacks. First, it can be applied only to VES curves on which there are no negative slopes that are equal to or less than $-1$, and second, it cannot be applied to VES curves that have positive slopes that are equal to or slightly greater than $+1$. There are several types of VES curves which have steeply descending branches with slopes of less than $-1$, and there are also field VES curves whose slopes may be slightly greater than $+1$ because of measurement errors or lateral in-

homogeneities. Furthermore, if the coordinates of two successive points on a branch of a VES curve, whose slope satisfies the relation $-1 \geq$ slope$\geq +1$, are used in equations 13 and 14, infinite or imaginary resistivities and thicknesses will be obtained. In order to overcome these difficulties we use MDZ (modified Dar Zarrouk) equations.

## MODIFIED DAR ZARROUK CURVES OF THE L TYPE

Figure 5 shows a theoretical three-layer VES curve of the H-type ($\rho_1 > \rho_2 < \rho_3$), its corresponding DZ curve, and the Hummel curve (Zohdy, 1965) for the conductive second layer. The steeply descending branch of the VES curve occupies an intermediate position between the descending DZ and Hummel curves. Therefore, for steeply descending branches on VES curves, there are curves, here called modified Dar Zarrouk curves of the L type (MDZ-L), which can be calculated from the combination of the DZ equations and the Hummel equations and which will approximate that steeply descending VES branch and lie close to it. Furthermore, when these MDZ-L curves are solved for layering, they will result in a geoelectric section which is equivalent to the section for which the VES curve was calculated or observed.

The parametric equations for MDZ-L curves are

$$\rho_{m_{L_j}} = \rho_{L_j} \left(\frac{\rho_{m_j}}{\rho_{L_j}}\right)^{X} = \frac{\sum_1^j h_i}{\sum_1^j S_i} \left[ \left( \frac{\sum_1^j T_i}{\sum_1^j S_i} \right)^{1/2} \Big/ \frac{\sum_1^j h_i}{\sum_1^j S_i} \right]^{X}, \qquad (18)$$

and

$$L_{m_{L_j}} = L_{L_j} \left(\frac{L_{m_j}}{L_{L_j}}\right)^{X} = \sum_1^j h_i \left[ \left( \sum_1^j T_i \sum_1^j S_i \right)^{1/2} \Big/ \sum_1^j h_i \right]^{X}, \qquad (19)$$

where

$\rho_{L_j}$ = average longitudinal resistivity, or Hummel resistivity, for the layers from 1 to $j$,

$L_{L_j} = \sum_1^j h_i$ = summation of layer thicknesses, or Hummel depth, to the bottom of the $j$th layer,

$X$ = number that lies in the interval $0 \leq X \leq 1$,

$S_i = h_i/\rho_i$ = longitudinal unit conductance of the $i$th layer,

$T_i = h_i\, \rho_i$ = transverse unit resistance of the $i$th layer.

For $X=1$, equations 18 and 19 reduce to the DZ equations 11 and 12, and for $X=0$ they reduce to the Hummel equations. For values of $0<X<1$, the MDZ-L curves occupy intermediate positions between the corresponding Hummel and DZ curves. The upper section of figure 6

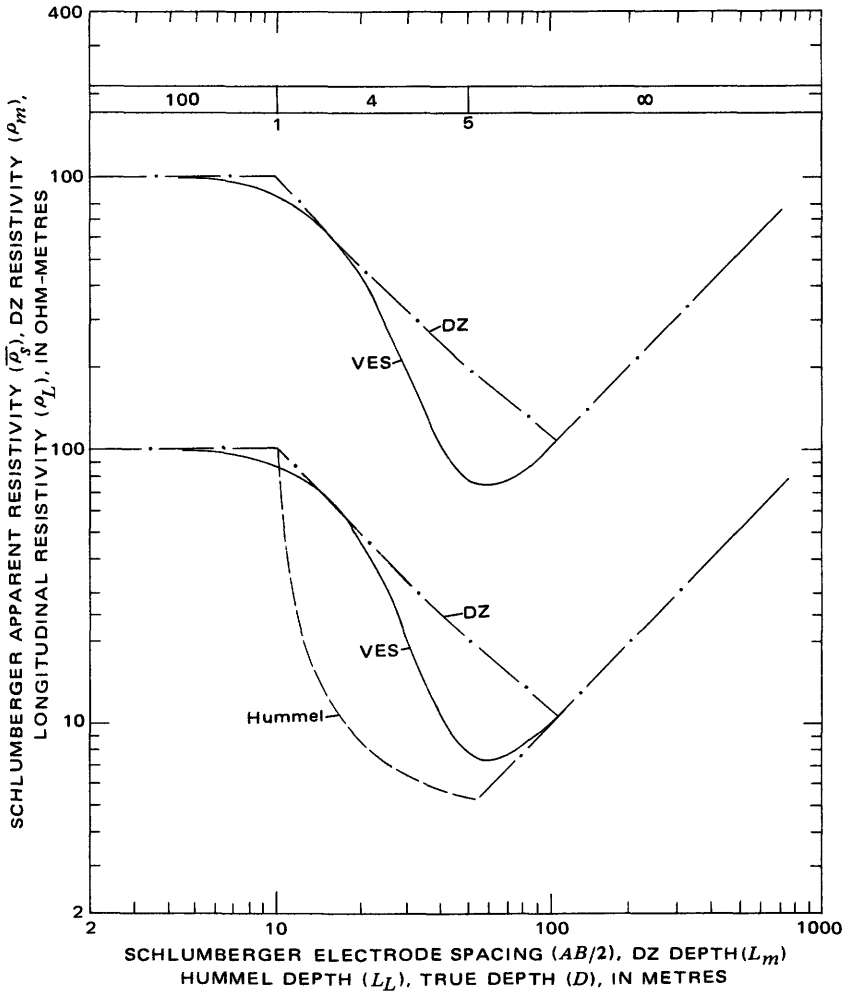


FIGURE 5. — Three-layer VES curve and corresponding DZ curve. Hummel curve is drawn for the conductive second layer only. Numbers in bar designate true resistivities in ohm-metres.

shows a set of MDZ–L curves computed for $\rho_2/\rho_1=0.01$ and various values of $X$. The lower section of figure 6 shows a set of MDZ–L curves calculated for $X=0.5$ and various values of the resistivity ratio $\rho_2/\rho_1$.

## INVERSION OF MDZ–L CURVES

The analytical expressions required for calculating the thickness and resistivity of a layer represented by two points on an MDZ–L curve are

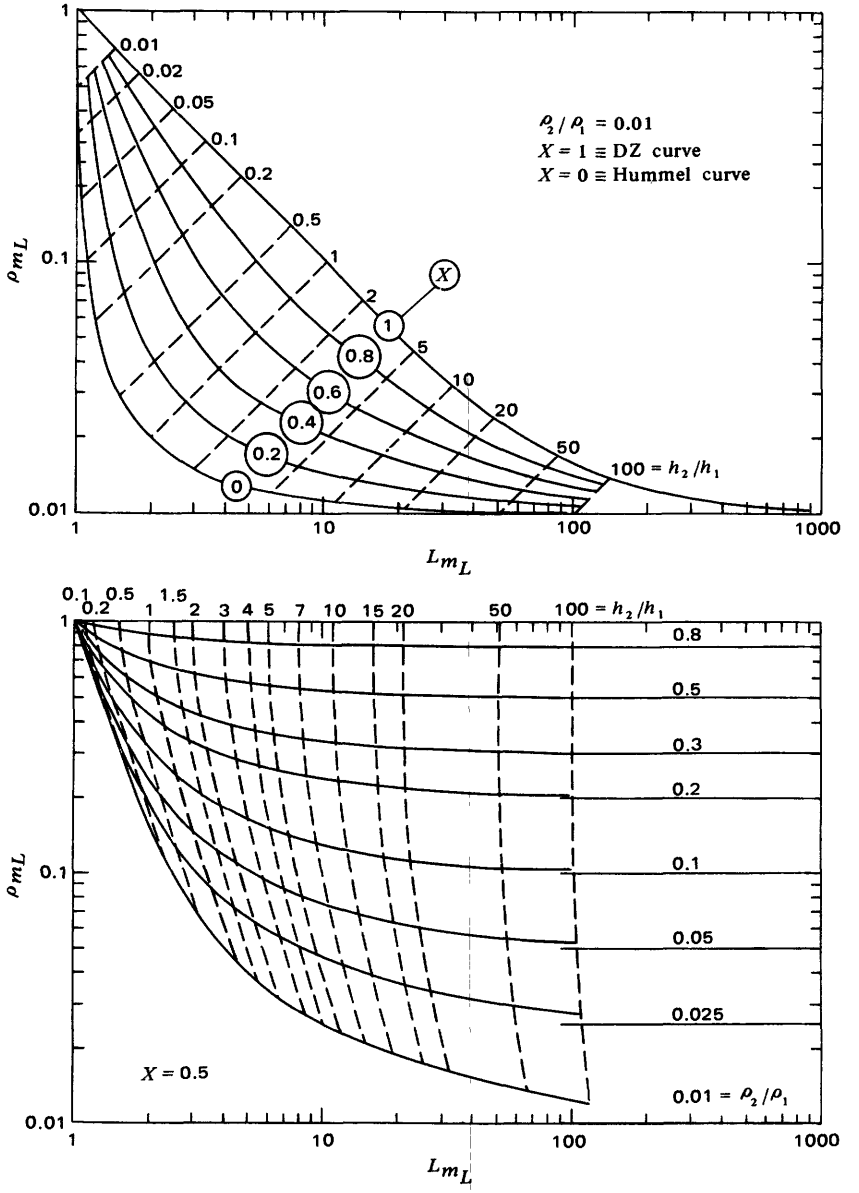


FIGURE 6. — Modified DZ curves of the L type. Top graph: MDZ-L curves for constant resistivity ratio $\rho_2/\rho_1$ and variable exponent $X$. Bottom graph: MDZ-L curves for constant value of the exponent $X=0.5$ and variable resistivity ratio $\rho_2/\rho_1$. $h_2/h_1$, thickness ratio; $\rho_{m_L}$, MDZ-L resistivity; $L_{m_L}$, MDZ-L depth.

derived as follows. Dividing equation 19 by equation 18 we get:

$$\frac{L_{m_{L_j}}}{\rho_{m_{L_j}}} = \sum_1^j S_i, \tag{20}$$

which indicates that the value of $S$ is preserved on MDZ-L curves (as it is preserved on Hummel and on DZ curves), and multiplying equation 18 by equation 19 we get

$$\rho_{m_{L_j}} L_{m_{L_j}} = \frac{\left(\sum_1^j h_i\right)^2}{\sum_1^j S_i} \left[\sum_1^j S_i \sum_1^j T_i \Big/ \left(\sum_1^j h_i\right)^2\right]^X. \tag{21}$$

For $j=1$ in equations 20 and 21, it can be shown that

$$\rho_{m_{L_1}} = \rho_1 \text{ and } L_{m_{L_1}} = h_1, \tag{22}$$

indicating that the coordinates $(L_{m_{L_1}}, \rho_{m_{L_1}})$ of the first point represent the thickness and the resistivity of the first layer, respectively. In a multilayer section, this first layer may be a fictitious layer that replaces all the overlying layers. For $j=2$ in equation 20, it follows, from equation 22, that

$$h_2 = \rho_2 \left(\frac{L_{m_{L_2}}}{\rho_{m_{L_2}}} - \frac{L_{m_{L_1}}}{\rho_{m_{L_1}}}\right). \tag{23}$$

The thickness of the second layer, $h_2$, can be calculated from equation 23 if its resistivity, $\rho_2$, has already been determined. The value of $\rho_2$ is calculated as follows. Substituting equations 22 and 23 in equation 21 for $n=2$, and simplifying to get

$$\left[\frac{L_j+\rho_2 Q}{L_{j+1}}\right]^2 \left[\frac{(L_j\tilde{\rho}_j+\rho_2 Q)}{(L_j+\rho_2 Q)^2} \cdot \frac{L_{j+1}}{\tilde{\rho}_{j+1}}\right]^X - 1 = 0, \tag{24}$$

where

$L_j$ and $L_{j+1} = L_{m_{L_j}}$ and $L_{m_{L_{j+1}}}$ = abscissas of two successive points on an MDZ-L curve,

$\tilde{\rho}_j$ and $\tilde{\rho}_{j+1} = \bar{\rho}_{m_{L_j}}$ and $\bar{\rho}_{m_{L_{j+1}}}$ = ordinates of two successive points on an MDZ-L curve,

$Q = (L_{j+1}/\tilde{\rho}_{j+1}) - (L_j/\tilde{\rho}_j)$,

$\rho_2$ = true resistivity of the second layer.

Equation 24 contains two unknowns: $X$ and $\rho_2$. In order to solve for $\rho_2$ at a given value of $0 \leq X \leq 1$ we use the iterative method known as the regula falsi method (Grove, 1966; Hildebrand, 1956).

The successful application of the regula falsi method relies on the ability of the user to assume two values for $\rho_2$, which, when consecutively substituted in the left-hand side of equation 24—here denoted by $f$—produce two values for $f$ with opposite algebraic signs. A negative value for $f$ indicates an underestimation of $\rho_2$, and a positive value for $f$ indicates an overestimation. Inasmuch as the resistivities in a physically acceptable model must be positive, the value of zero for $\rho_2$ must be made to represent an underestimation of the true value of $\rho_2$. Therefore, with $X=1$ (DZ equation) and $\rho_2=0$ in equation 24, if the value of $f$ is positive, then the value of $f$ must be forced to become negative by decrementing the value of the exponent $X$, from 1 to 0. With $X=0$ and $\rho_2=0$, the value of $f$ will always be negative as it can be readily proved from equation 24. As shown by the comparison of figures 5 and 6, MDZ–L curves for $X\cong 0.5$ approximate steeply descending VES branches better than DZ curves ($X=1$) or Hummel curves ($X=0$). Therefore, to approximate descending VES branches, the "first" value of $X$ is generally taken as 0.6, and, if $f$ is positive, then $X$ is decremented by 0.2 ($X=0.6$, 0.4, 0.2, 0). The first value of $X$ and the rate at which it is decremented affect the thicknesses and resistivities of the layers to be obtained from the inversion.

By assuming $\rho_2=\tilde{\rho}_{i+1}$, a positive value of $f$, $f_+$, always is obtained because, on a descending MDZ–L branch (for any value of $0\leq X\leq 1$), the MDZ–L resistivity $\tilde{\rho}_{i+1}$ always is greater than $\rho_2$ except at the asymptote where $\tilde{\rho}_{i+1}=\rho_2$, if $\tilde{\rho}_{i+1}=\rho_2$, then the value of $f$ is zero, and the required value of $\rho_2$ is determined.

Having determined the first value for $X=X'$ (where $0\leq X'\leq 0.6$), for which $f=f_-$ at $\rho_2=\rho_{2-}=0$, and using $\rho_{2+}=\tilde{\rho}_{i+1}$ to calculate $f=f_+$ at $X=X'$, we use the iterative regula falsi equation to calculate the first approximation for $\rho_2$ from

$$\rho_2(1)=\frac{\rho_{2-}f_+-\rho_{2+}f_-}{f_--f_+}. \tag{25}$$

We substitute $\rho_2$ (1) for $\rho_2$ in equation 24 to calculate $f_-$ (1), then we substitute $\rho_2$ (1) and $f_-$ (1) for $\rho_2$ and f_ in equation 25 to calculate the second approximation for $\rho_2=\rho_2$ (2). The iteration is repeated for a maximum of 15 times or until

$$0.98\leq\frac{\rho_2(i)}{\rho^2(i-1)}\leq 1.02. \tag{26}$$

Having determined the value of $\rho_2$, by the above iterative method we can calculate the thickness, $h_2$, from equation 23.

To summarize, for the automatic interpretation of VES curves, ascending branches on VES curves are approximated by DZ curves and descending branches are approximated by MDZ–L curves. The

iterative formula 15 is used for calculating the ordinates of the successive DZ and MDZ–L points whose inversions successively approximate the required solution.

## MODIFIED DAR ZARROUK CURVES OF THE T TYPE

A theoretical VES curve for horizontally stratified, laterally homogeneous media may have a rising branch with a slope of +1, which reflects the detection of a layer with an infinitely large resistivity; in practice, field VES curves may have slopes that are slightly, or significantly, greater than +1. Such slopes may be caused by lateral heterogeneities (Kalenov, 1957), fences with metal posts, errors in measurements, or current leakage (Zohdy, 1968). Furthermore, in applying the iterative equation 15 for adjusting the ordinates of DZ and MDZ–L curves, it is possible that the slope between two successive points may become $\geq 1$ after several iterations have been made. If the ordinates of points on such steeply ascending segments are used in the DZ inversion equations, infinite or imaginary resistivities and thicknesses will be obtained.

To overcome this problem, we define MDZ–T curves whose parametric equations are given by

$$\rho_{m_{t_j}} = \rho_{t_j}\left(\frac{\rho_{m_j}}{\rho_{t_j}}\right)^X = \frac{\sum_1^j T_i}{\sum_1^j h_i}\left[\frac{\sum_1^j h_i}{\sum_1^j T_i}\left(\frac{\sum_1^j T_i}{\sum_1^j S_i}\right)^{1/2}\right]^X, \tag{27}$$

and

$$L_{m_{t_j}} = L_{t_j}\left(\frac{L_{m_j}}{L_{t_j}}\right)^X = \sum_1^j h_i\left[\frac{\left(\sum_1^j T_i \sum_1^j S_i\right)^{1/2}}{\sum_1^j h_i}\right]^X, \tag{28}$$

where

$\rho_{t_j} = \sum_1^j T_i / \Sigma h_i$ = average transverse resistivity of the layers from 1 to $j$,

$L_{t_j} = \Sigma h_i$ = summation of layer thickness to the bottom of the $j$th layer,

$X$ = number that lies in the interval $0 \leq X \leq 1$.

Equations 27 and 28 are similar to equations 18 and 19 except that $\rho_t$, instead of $\rho_L$, is used to modify the DZ resistivities and depths. Depending on the value of $X$ and on the parameters of the section, the corresponding MDZ–T curve can have slopes that are greater than 1. In fact, the MDZ–T curves (fig. 7) look almost like a mirror image of MDZ–L curves (fig. 6) reflected across the abscissa.

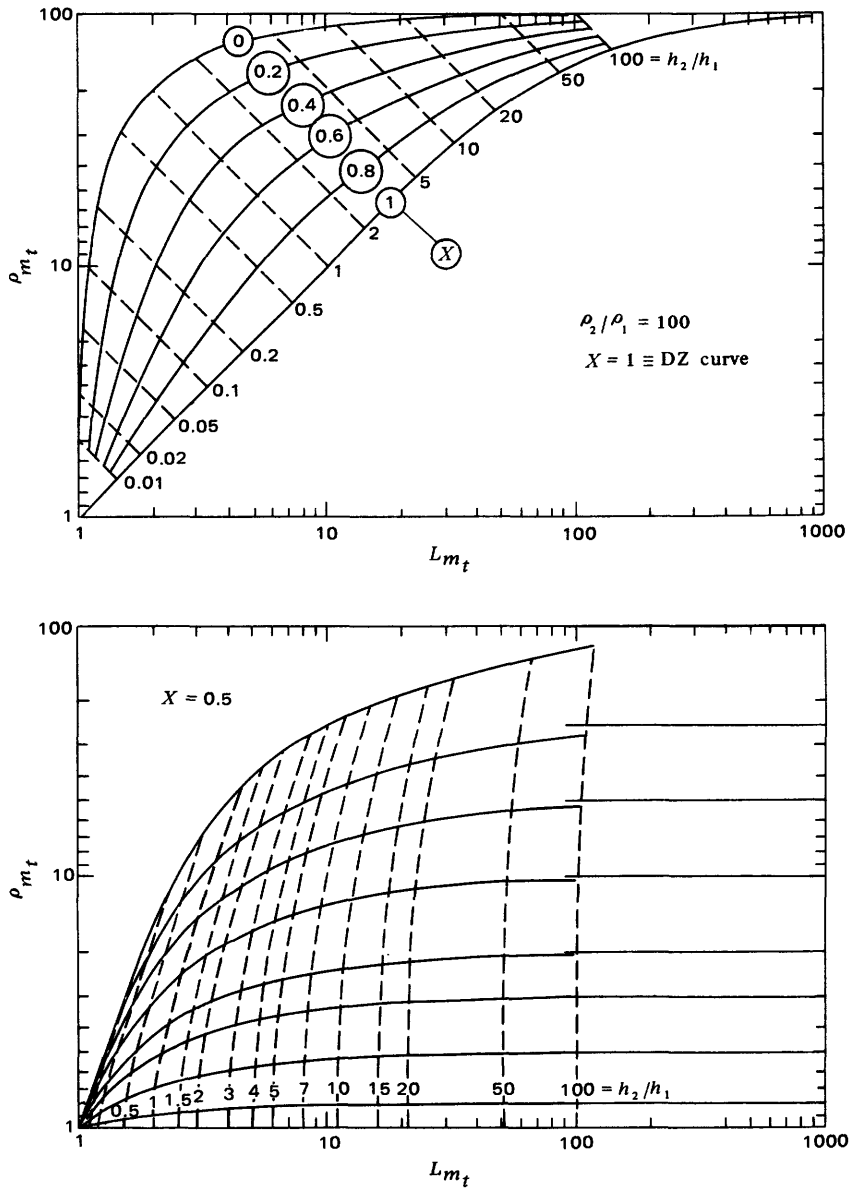


FIGURE 7. — Modified DZ curves of the T type (MDZ-T). Top graph: MDZ-T curves for constant resistivity ratio $\rho_2/\rho_1$ and variable exponent $X$. Bottom graph: MDZ-T curves for constant value of the exponent $X=0.5$ and variable resistivity ratio $\rho_2/\rho_1$. $h_2/h_1$, thickness ratio; $\rho_{m_t}$, MDZ-T resistivity; $L_{m_t}$, MDZ-T depth.

## INVERSION OF MDZ-T CURVES

The equations for the inversion of MDZ–T curves are similar to those for the inversion of MDZ–L curves and are derived as follows. Multiplying equation 27 by 28 we get

$$\rho_{m_{t_j}} L_{m_{t_j}} = \sum_1^j T_i , \tag{29}$$

which indicates that the values of T are preserved on MDZ–T curves. Dividing equation 27 by equation 28 we get

$$\frac{\rho_{m_{t_j}}}{L_{m_{t_j}}} = \frac{\sum_1^j T_i}{\left(\sum_1^j h_i\right)^2} \left[ \frac{\left(\sum_1^j h_i\right)^2}{\sum_1^j T_i \sum_1^j S_i} \right]^X , \tag{30}$$

For $i=1$ in equation 27 and 28, it can be shown that

$$\rho_{m_{t_1}} = \rho_1 \text{ and } L_{m_{t_1}} = h_1, \tag{31}$$

and for $j=2$ in equation 30, it follows, from equations 29 and 31 that

$$h_2 = \frac{\rho_{m_{t_2}} L_{m_{t_2}} - \rho_{m_{t_1}} L_{m_{t_1}}}{\rho_2} . \tag{32}$$

substituting equation 31 and 32 in equation 30 for $j=2$, and simplifying we get

$$\frac{L_{j+1}}{\left[L_j + \frac{K}{\rho_2}\right]^2} \cdot \left[ \frac{\left(L_j + \frac{K}{\rho_2}\right)^2}{L_{j+1} \tilde{\rho}_{j+1} \left(\frac{L_1}{\tilde{\rho}_j} + \frac{K}{\rho_2^2}\right)} \right] - 1 = 0, \tag{33}$$

where

$K = \rho_{m_{t_j}} L_{m_{t_j}} - \rho_{m_{t\,j-1}} L_{m_{t\,j-1}}$,

$L_j$ and $L_{j+1} = L_{m_{t_j}}$ and $L_{m_{t_{j+1}}}$,

$\tilde{\rho}_j$ and $\tilde{\rho}_{j+1} = \rho_{m_{t_j}}$ and $\rho_{m_{t_{j+1}}}$ and

$\rho_2$ = true resistivity of the second layer.

Equation 33 is analogous to equation 24 and can be solved for $\rho_2$, using the regula falsi method. For an underestimation of $\rho_2$ we set $\rho_2 = \tilde{\rho}_{i+1}$, and for an overestimation of $\rho_2$, we set $\rho_2 = 50\,\tilde{\rho}_{i+1}$. The equation is tested with $\rho_2 = 50\,\tilde{\rho}_{i+1}$ and $X = 1, 0.9, 0.8, \ldots$ and so on, in search of a positive value for the left-hand side, which would indicate that $\rho_2 = 50\,\tilde{\rho}_{i+1}$ is an overestimation. Then, having guaranteed that the appropriate value of $X$ has been determined for a positive value of $\rho_2$, we

proceed to use the regula falsi method for evaluating $\rho_2$ and, hence, $h_2$ from equation 32.

## INVERSION OF VES CURVES

The inversion of a Schlumberger VES curve is made by finding an MDZ curve (which may be formed of a combination of DZ, MDZ–L, and MDZ–T segments) which lies close to the observed VES curve and whose inversion results in a layering for which a calculated VES curve practically coincides with the observed VES curve. The slopes at the successive points on the digitized VES curve are calculated using the formula

$$SLOPE_{i+1}=\log\left(\bar{\rho}_{s_{i+1}}/\bar{\rho}_{s_i}\right)/\log\left(L_{i+1}L_i\right), \tag{34}$$

where $L=AB/2$=Schlumberger electrode spacing, and $i=1, \ldots, n$. Equation 34 assigns the value of the slope between the $i$th and $(i+1)$ point to the $(i+1)$ point. The slope of the first point is assumed to be equal to zero.

There are at least two advantages for the computation of these slopes:
1. If the slope exceeds +1, the computer will print a warning message about the distortion of the VES curve, and if the slope exceeds the arbitrarily set value of 1.4, then this generally indicates that an error in punching or digitizing the data has been made, and the problem is automatically rejected by the computer unless it was specifically instructed to find the best fitting curve regardless of curve distortions.
2. The fitting tolerance, $FT$, for each point on the observed VES curve, is defined in terms of the slope by the formula

$$FT_i=M+N\ (SLOPE_i)^2, \tag{35}$$

where $M$ and $N$ are usually taken equal to 5 and 1, respectively. The fitting tolerance for the first point is arbitrarily assigned the value of 5. Equation 35 allows a larger fitting tolerance for steeply descending branches than for moderately descending or ascending branches.

The computer compares the values of the successive ordinates on the digitized VES curve and, for each pair of successive points, it decides, on the basis of the value of $\rho_{m_{i+1}}/\rho_{m_i}$, whether the DZ, MDZ–L, or MDZ–T inversion equations should be used. By applying the appropriate inversion formulas, we obtain a geoelectric layering in which the number of layers is equal to the number of points on the digitized VES curve. The thickness of the last layer is set to equal a very large number (9999999).

The TKF curve is calculated for this layering using Sunde's recursion formula and a VES curve is calculated by convolution using Ghosh's inverse filter coefficients, so that the abscissas of the calculated and observed VES points are the same. The percentage

difference, $PD$, between calculated $\bar{\rho}_c$, and observed, $\bar{\rho}_0$, apparent resistivity values is calculated from

$$PD_i = \left| \frac{\log \bar{\rho}_{0_i} - \log \bar{\rho}_{c_i}}{\log \bar{\rho}_{0_i}} \right| \times 100.$$

The sum of the squared residuals (SSQR)

$$SSQR = \sum_{i=1}^{N} \left[ \log \bar{\rho}_{0_i} - \log \bar{\rho}_{c_i} \right]^2$$

is also calculated.

If the percentage difference for one calculated point exceeds its precalculated fitting tolerance, the iterative equation 15 is used to calculate the ordinates of a new set of MDZ points. This newly constructed MDZ curve is inverted, and a second VES curve is calculated. If a match between observed and calculated VES curves (within the prescribed fitting tolerance for each point) is not obtained after 10 iterations (using equation 15), or if the sum of the squared residuals increases 5 times, instead of decreasing, then the layering solution with the least SSQR is saved in the computer.

The failure of the iterative procedure to produce a satisfactory match between observed and calculated VES curves indicates one or both of the following possibilities:

1. The curve is distorted and therefore it may be impossible to fit every point on it with a theoretical curve, which is calculated for horizontal layering.
2. The left branch of the curve is incomplete, and (because, in the iterative procedure, only the ordinate of the first point is allowed to change and not its abscissa) it is impossible to fit the curve with a model in which the thickness of the first layer is equal to the electrode spacing of the first point. This problem can be solved if the thickness of the first layer is forced to become less than the abscissa of the first point on the curve.

Therefore, we introduce the concept of the thickness reduction factor $0<y\leq 1$, which is multiplied by the value of the thicknesses $h_1$ and $h_2$ after their calculation from equations 14, 23, or 32. Thus, for the first set of iterations, the value of the thickness reduction factor, $y$, is set equal to unity. If this does not result in a satisfactory match, then, with the value of $y$ decreased by an decrement of 0.1, the whole iterative procedure is repeated from the start. For each set of iterations, with a fixed value of $y$, the least $SSQR$ obtained is compared with the one obtained from the previous set of iterations. If the value of the least $SSQR$ for one set of iterations becomes larger than that of the previous set of iterations, the automatic inversion procedure is terminated and the solution with the least $SSQR$ is printed. The maximum number of

allowed iterations is set to equal 60 (which implies that the value of $y$ is allowed to decrease a maximum of 5 times).

Figure 8 shows the output of five iterations from the first set of iterations (in which the value of $y$ is equal to unity) for the automatic interpretation of a theoretical three-layer curve of the H type. In step 1 the sought MDZ curve is approximated by the observed $VES_0$ curve itself ($MDZ_1 = VES_0$). The inversion of this $MDZ_1$ curve and subsequent calculation of the apparent resistivities result in the $VES_1$ curve. The ordinates of the $VES_0$ and $VES_1$ curves are compared and the ordinates of the second approximation ($MDZ_2$) for the MDZ curve are calculated from equation 15 which is symbolized differently (from equation 15) on the figure ($\bar{\rho}_{s_0} = VES_0$, $\bar{\rho}_{s_i} = VES_i$, $\bar{\rho}_{m_i} = MDZ_i$, and $\rho_{m_{i+1}} = MDZ_{i+1}$). The iteration is continued through step 5 where the curve of $VES_5$, which is calculated for the layering obtained from the inversion of the $MDZ_5$ curve, practically coincides with the curve of $VES_0$. In this example, $VES_1$ through $VES_5$ were calculated by numerical integration rather than by convolution.

The number of layers in the resulting model is equal to the number of points on the digitized curve. This model constitutes the detailed solution, which, for the example under consideration, is composed of 15 layers. In the detailed solution, some successive layers may have almost the same resistivity and, therefore, the actual number of layers with distinctly different resistivities may be less than the number of points on the curve. In this example the number of such distinct layers is nine. It is important to realize that had the reference VES curve been calculated or observed over these nine layers, then its interpretation, by conventional curve-matching methods, would have been made in terms of the three-layer model.

Figure 9 shows the DZ curves and the layering distributions for both the automatically obtained nine-layer model and the original theoretical three-layer model. The resistivities of the infinitely thick bottom layers on the two models are different because the last branch on the $VES_0$ curve is not well developed and was not plotted to the point at which it asymptotically would have approached the value of the true resistivity of the bottom layer. Nevertheless, this example illustrates the fact that the application of the method does not depend on the extension and full development of the last branch on the observed VES curve, which is a requirement for the other methods of automatic interpretation that use the transformation of VES curves into their corresponding total-kernel-function curves by convolution (Strakhov and Karelina, 1969; Ghosh, 1971a). The development of the first branch on the observed VES curve, at least to electrode spacings that are equal to or less than the thickness of the first layer, is recommended but not required.

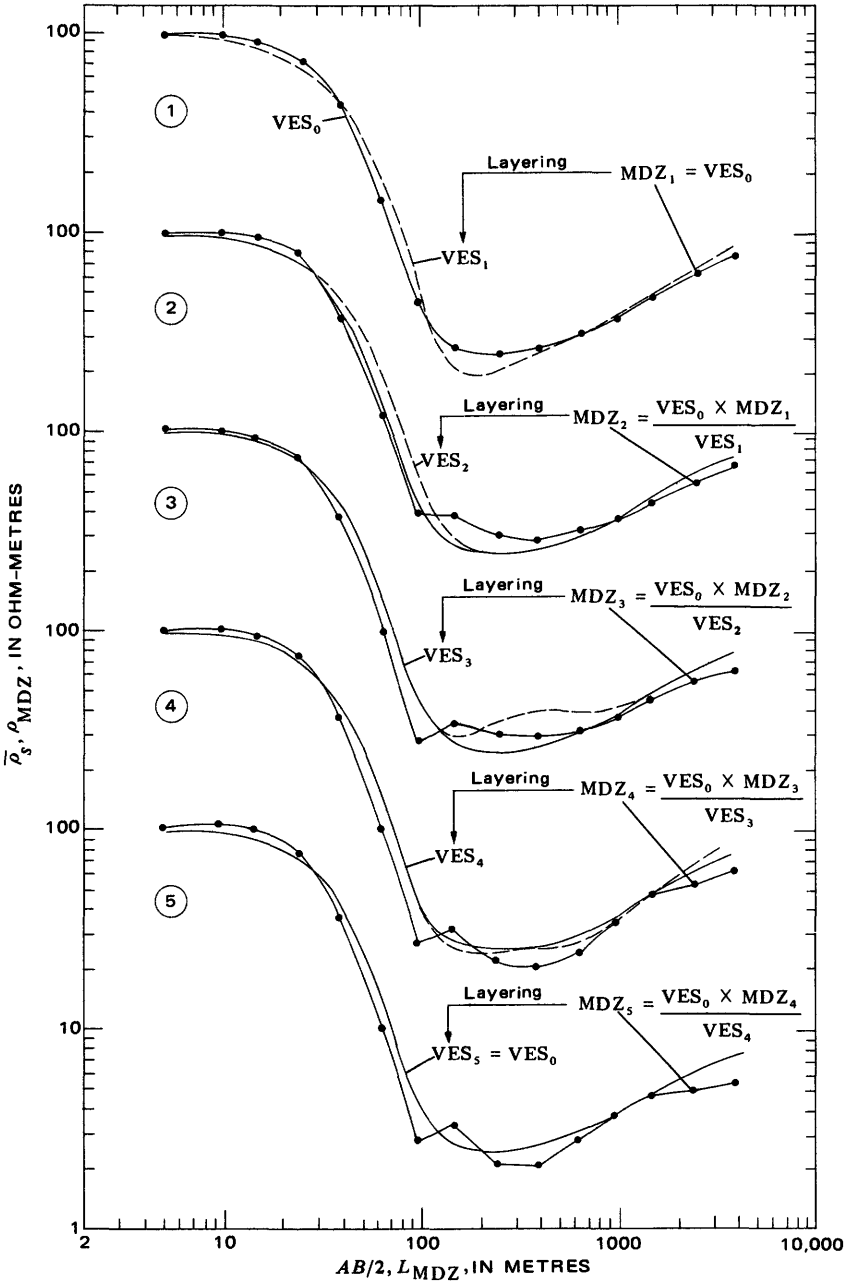
100
100
100
100
100
10
1
2
10
100
1000
10,000
1
2
3
4
5
VES$_0$
Layering
MDZ$_1$ = VES$_0$
VES$_1$
Layering
MDZ$_2$ = VES$_0$ × MDZ$_1$ / VES$_1$
VES$_2$
Layering
MDZ$_3$ = VES$_0$ × MDZ$_2$ / VES$_2$
VES$_3$
Layering
MDZ$_4$ = VES$_0$ × MDZ$_3$ / VES$_3$
VES$_4$
Layering
MDZ$_5$ = VES$_0$ × MDZ$_4$ / VES$_4$
VES$_5$ = VES$_0$
$\bar{\rho}_s$, $\rho_{MDZ}$, IN OHM-METRES
$AB/2$, $L_{MDZ}$, IN METRES

◁ FIGURE 8. — Curves showing the output of five iterations for the inversion of a theoretical three-layer VES curve of the H type. $VES_0$, reference VES curve or ordinates on $VES_0$ curve; $MDZ_1$ to $MDZ_5$, successive approximations to ordinates of MDZ curve; $VES_1$ to $VES_5$, VES curves calculated for the layering obtained from the inversion of $MDZ_1$ to $MDZ_5$ curves, respectively. $\rho_{MDZ}$, MDZ resistivity; $L_{MDZ}$, MDZ depth; $\bar{\rho}_s$, Schlumberger apparent resistivity; $AB/2$, Schlumberger electrode spacing.

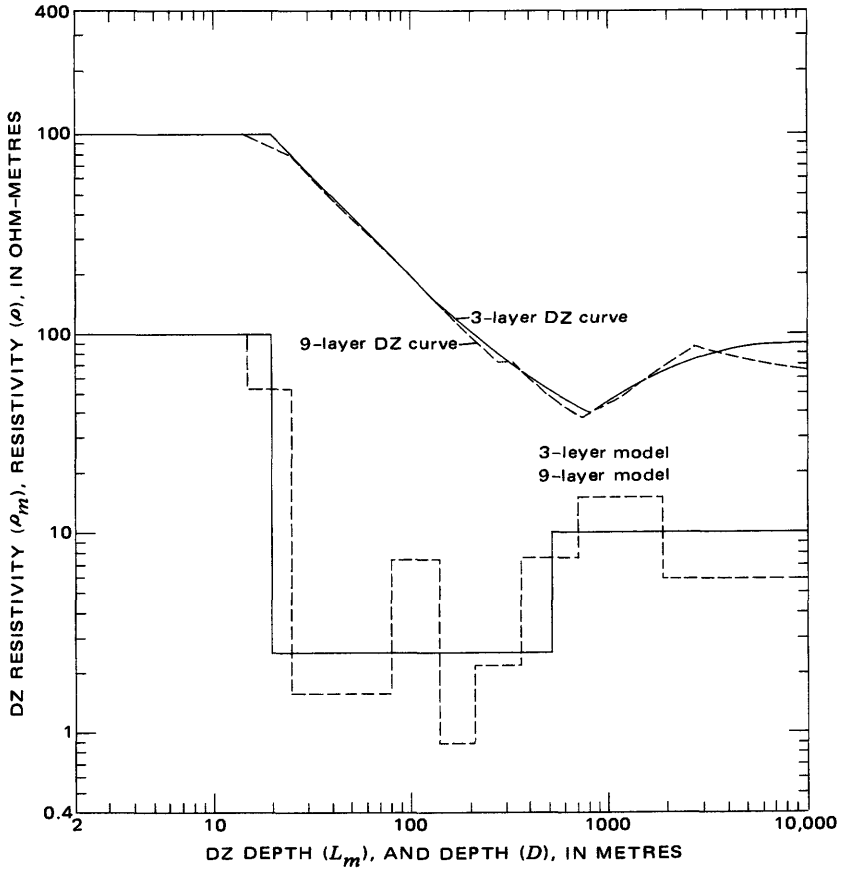


FIGURE 9. — Comparison between equivalent DZ curves and equivalent layering for reference theoretical three-layer model and automatically obtained nine-layer model.

## INVERSION OF INCOMPLETE AND (OR) DISTORTED VES CURVES

Incomplete VES curves are here defined as VES curves on which neither the left branch nor the right branch forms asymptotes to the first- and last-layer resistivities, respectively. However, a VES curve whose right branch rises at an angle of 45° and is defined by at least three points extending over about one-third of a logarithmic cycle is considered as having a complete terminal branch.

In contrast to other automatic or semiautomatic methods of interpretation, the method presented here does not rely on the completeness of the first and terminal branches of the observed curve. The problem created by the incompleteness of the left branch is overcome by introducing the thickness reduction factor, $y$, mentioned earlier, and the problem of the incompleteness of the right VES branch is simple to resolve by using the MDZ method and setting the thickness of the last layer equal to a very large number. However, when the right branch on the VES curve is incomplete, the automatically interpreted model may show a resistivity for the last layer which is different from the resistivity anticipated by the interpreter; nevertheless, all the given points on the observed curve would be properly fitted. Therefore, if the interpreter has any preconceived notions about the resistivity of the last layer, then he should extrapolate the terminal branch toward its assumed asymptote.

Although the completeness of the first (left) branch is not a requirement for the applicability of the computer program (Zohdy, 1974c), it simplifies the problem, and a few seconds of computer time may be saved.

Distorted VES curves are defined here as VES curves whose curvature at certain points cannot be fitted with theoretical VES curves which are calculated for horizontally stratified media. The distortion on a VES curve may be caused by inhomogeneities in the horizontal direction or by errors in measurement or may even be created by errors in digitizing the data for an otherwise smooth VES curve. If the distortion on a given VES curve is such that the logarithmic slope on the curve at any given point exceeds 1.4, then, as mentioned earlier, the computer automatically rejects the problem unless it was instructed not to. If, however, the distortion on the VES curve is more moderate, then the automatic interpretation program will yield a calculated VES curve which fits the digitized points in the least-square sense, although not necessarily within the prescribed fitting tolerance.

In attempting, even though unsuccessfully, to fit all the given points on a distorted VES curve, the detailed layering may contain a geologically improbable sequence of thin layers with highly contrasting resistivities. Consequently, the calculated VES curve for the

improbable layering (which fits the distorted VES curve in the least-square sense) is considered as a smoothed version of the observed curve and is automatically reinterpreted to obtain a more realistic layering.

In the reinterpreted model, the replacement of the sequence of layers having highly contrasting resistivities by a sequence of layers having more moderately contrasting resistivities shows that the layers with highly contrasting resistivities were not only geologically improbable but also geoelectrically unnecessary; if their presence was accurately reflected on the calculated VES curve before reinterpretation, then, most likely, they would have been obtained also in the reinterpreted model.

The computer program is written so that if one point on the digitized observed VES curve cannot be fitted within the prescribed fitting tolerance, then the detailed solution for which $\Sigma[\log\bar{\rho}_0 - \log\bar{\rho}_c]^2 =$ minimum is chosen. The VES curve for this detailed model is recalculated, starting at an electrode spacing equal to one-tenth the smallest given electrode spacing and, if specified by the user, ending at an electrode spacing equal to ten times the largest given electrode spacing (thus generating a complete VES curve if the given curve was incomplete as well as distorted). This new VES curve, which is complete and smooth, is automatically reinterpreted. The number of layers in the detailed model is reduced through the automatic smoothing of the corresponding DZ curve.

Figure 10 shows an example of the interpretation of an incomplete and distorted VES curve. The layering shown in figure 10*A* contains an unrealistic sequence of thin layers, with resistivities ranging from 1.05 to about 2,600 ohm-metres. These layers were created primarily in attempting to fit the incomplete left branch of the curve and the distorted segment on the VES curve between the electrode spacing of 100 and 1,000 m (metres).

Figure 10*B* shows the DZ curve for the unrealistic detailed model. The fundamental DZ points occurring at the DZ depths of about 75, 110, and 172 m, respectively, cannot be easily smoothed by using the automatic procedures to be described later, although they can be smoothed manually.

Figure 10*C* shows the complete VES curve (starting at the electrode spacing of $AB/2$ = 1 m and terminating at $AB/2$ = 10,000 m calculated for the unrealistic detailed model shown in figure 10*A*. This VES curve (which now may be considered as the complete and smoothed version of the observed curve) was automatically interpreted in terms of the realistic detailed layering also shown in figure 10*C*; the VES curve calculated for this layering is shown in the graph with the open circles.

Figure 10*D* shows the detailed DZ curve for the 25 layers in figure 10*C* and the fundamental DZ points (1–6) which were obtained using the

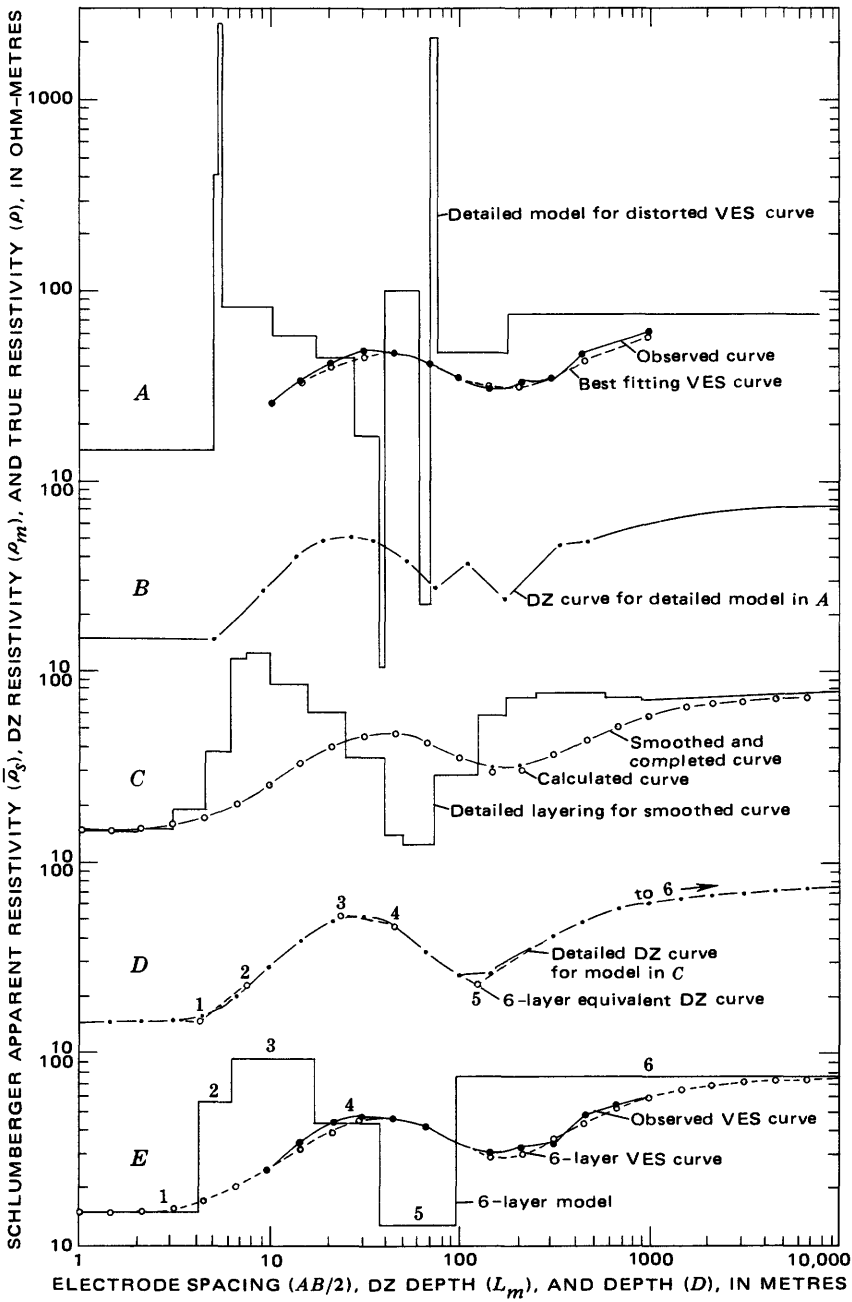


FIGURE 10. — Graphs showing the automatic interpretation of an incomplete and distorted VES curve.

automatic-DZ-smoothing subroutine (Zohdy, 1974c). The automatic inversion of the smoothed DZ curve resulted in the six-layer model shown in figure 10*E*, where the corresponding six-layer VES curve is compared with the original digitized data of the observed curve.

## AUTOMATIC SMOOTHING AND INVERSION OF DZ CURVES

The number of layers in the detailed model obtained from the automatic interpretation can be reduced automatically so that the resulting model will contain only the fundamental layers in the geoelectric section, and so that the reduced model will be electrically equivalent to the detailed model. The number of layers is reduced by first calculating the DZ curve for the detailed model, then smoothing it numerically and inverting it. The following two methods were devised for smoothing the detailed DZ curve.

### 1. FIRST METHOD

In this first method the fundamental DZ points designating the termination of one fundamental DZ branch and the beginning of another are also points on the detailed DZ curve. By successively substituting the coordinates of the first DZ point ($L_{m_1}$, $\rho_{m_1}$), which is taken as the first fundamental DZ point, and the coordinates of the successive points ($L_{m_2}$, $\rho_{m_2}$), ($L_{m_3}$, $\rho_{m_3}$), . . . , ($L_{m_k}$, $\rho_{m_k}$) in the inversion equation

$$\rho_2{}^*{}_k = \sqrt{\frac{L_{m_k}\rho_{m_k} - L_{m_1}\rho_{m_1}}{\frac{L_{m_k}}{\rho_{m_k}} - \frac{L_{m_1}}{\rho_{m_1}}}}, \tag{36}$$

we can solve for a succession of second-layer resistivities, $\rho_2{}^*$. Each time a value for $\rho_2{}^*$ is calculated, we use the equation (Zohdy, 1974a)

$$\rho_{m_c} = \frac{-L_{m_1}\left(\rho_{2k}{}^2 - \rho_{m_1}{}^2\right) + \sqrt{\left(L_{m_1}\left(\rho_{2k}{}^2 - \rho_{m_1}{}^2\right)\right)^2 + 4\left(L_{m_i}L_{m_1}\rho_{2k}\right)^2}}{2\,L_{m_i}\rho_{m_1}} \tag{37}$$

to calculate $\rho_{m_c}$ values at the abscissas $L_{m_i}$, which lie between $L_{m_1}$ and $L_{m_k}$. We calculate the ratio $\rho_{m_c}/\rho_m$ to evaluate the deviations of the ordinates on the calculated two-layer DZ curve from the ordinates ($\rho_m$) of points on the detailed DZ curve. If, upon using the coordinates of the ($I$+1) point on the detailed DZ curve, the ratio $\rho_{m_c}/\rho_m$, for any point between 1 and ($I$+1), exceeds 1.05 or becomes less than 0.95, the ($I$+1) point is dropped and the coordinates of the $i$th point on the detailed DZ curve are taken as the coordinates of the second fundamental DZ point.

The above procedure is repeated with the last-determined fundamental DZ point taken as the starting point. When the $n$th point on the detailed DZ curve has been used, the smoothing procedure is terminated, and the coordinates of the fundamental DZ points are used in the inversion equations 13 and 14 to calculate the reduced layering.

### 2. SECOND METHOD

This method is based in part on applying the method of least squares to the linear representation of DZ curves, which is a plot of $T$ as a function of $S$. For a homogeneous and isotropic earth, the curve $T=f(S)$ is a straight line. This can be shown by considering the following equations. For an inhomogeneous earth,

$$T=\rho_1 h_1+\rho_2 h_2+\ldots+\rho_n h_n=\rho_t H, \tag{38}$$

$$S=\frac{h_1}{\rho_1}+\frac{h_2}{\rho_2}+\ldots+\frac{h_n}{\rho_n}=\frac{H}{\rho_L}, \tag{39}$$

$$T=\rho_t \rho_L S, \tag{40}$$

but, for a homogeneous earth, $\rho_t=\rho_L=\rho$, and, therefore,

$$T=\rho^2 S, \tag{41}$$

which is the equation of a straight line whose slope is equal to the square of the resistivity of the medium.

In bilogarithmic presentation the first fundamental DZ branch $(\rho_m=f(L_m))$ is a horizontal line; preferably the smoothing process for the first fundamental branch is made by successively averaging the ordinates of the successive DZ points on the $n$-layer DZ curve, using the formula

$$\rho_m^*(I)=e^{\sum_{i=1}^{I} \ln \rho_{m_i}/I}, \tag{42}$$

where

$i=1, 2, \ldots =$successive number of points,

$I=$number of averaged points, and

$\rho_m^*(I)=$average value of $\rho_m$ in the logarithmic sense.

The successive deviations

$$\delta_i(I)=\rho_{m_i}/\rho_m^*(I) \tag{43}$$

are calculated, and if with the inclusion of the $(I+1)$ point the value of $\delta_i(I+1)$, for any value of $1\leq i\leq I+1$, is greater than 1.05 or smaller than 0.95, the averaging process is terminated, and the value of $\rho_m(I)$ is taken as equal to $\rho_1$, which is the average true resistivity for the "first" layer.

In linear presentation of DZ curves, the general equation for the first straight line is

$$T_1 = A_{01} + A_{11} S_1, \tag{44}$$

where $A_{01} = 0$, and $A_{11} = \rho_1^{*2}$ (see equation 41). Starting at the last point that was included in the above logarithmic averaging process, we successively use the least-squares equations

$$A_1 = \frac{I\Sigma(TS) - \Sigma T \cdot \Sigma S}{I\Sigma S^2 - (\Sigma S)^2}, \tag{45}$$

$$A_0 = \frac{\Sigma T - A_1 \Sigma S}{I}, \tag{46}$$

where $T = \Sigma T_i$, $S = \Sigma S_i$, and $I$ = number of points used, to compute the successive coefficients $A_0$ and $A_1$ of a succession of the straight lines:

$$T_2(I) = A_{02}(I) + A_{12}(I) S_2(I). \tag{47}$$

The abscissas ($S$) and ordinates ($T$) of the intersections of these successive straight lines with the first straight line are calculated successively from the equations

$$S_1 = \frac{A_{02}(I) - A_{01}}{A_{11} - A_{12}(I)}, \tag{48}$$

$$T_1 = A_{01} + A_{11} S_1. \tag{49}$$

Equations 48 and 49 are obtained by the simultaneous solution of equations 44 and 47 for $T_1 = T_2$ and $S_1 = S_2$.

The number of points, $I$, to be included on any given $T = f(S)$ straight line or DZ branch is governed by the following conditions:

1. If, upon the inclusion of $(I+1)$ point for the $J$th line, the value of the slope $(A_{1,J})$ becomes negative or zero, an imaginary or zero resistivity $(\rho_J^* = \sqrt{A_{1,J}})$ is obtained and the $(I+1)$ point is dropped.
2. If, upon the inclusion of the $(I+1)$ point on the $J$th line, the intersection of the $J$th and $(J-1)$ lines occurs at an abscissa value less than the abscissa of the point preceding the last point on the $(J-1)$ line or greater than the abscissa of the point succeeding the last point on the $(J-1)$ line, then the $(I+1)$ point is dropped.
3. If, in condition 2 above $I+1=2$, then the coordinates $T$ and $S$ of the first point on the $J$th line (which are also the coordinates of the last point that was averaged on the $J-1$ line) are redefined in terms of $T$ and $S$ of the corresponding point on the smoothed $(J-1)$ line. This will guarantee that the coordinates of the point of intersection of $(J-1)$ line and the $J$th line are the same as the coordinates of the last point on the smoothed $(J-1)$ line.

4. If, upon the inclusion of the $(I+1)$ point, the fitting tolerance for any point $1 \leq i \leq (I+1)$ is exceeded, then, again, the $(I+1)$ point is dropped.

The fitting tolerance (in condition 4) is here defined in terms of the slopes, $s_i$, of the points on the two-layer DZ curves (bilogarithmic presentation) which are used to fit the fundamental segments on the $n$-layer DZ curve. The following equation is used to define the fitting tolerance:

$$K_i = a\left[2+s_i\right]\left[\cos\left(\frac{\pi s_i}{2}\right)\right]/10\,, \tag{50}$$

where

$a$ = a number set equal to 2, 4, or 8,

$s_i$ = slope of the $i$th point on the two layer DZ curve.

A plot of the function $K_i = f(s_i)$ for a = 1.5, 2, 2.5, and 3 is shown in figure 11 and indicates that the fitting tolerance generally is larger for positive values of $s_i$ than for negative values of $s_i$. This property makes the function $K$ suitable for defining the fitting tolerance in accordance with the rules governing the equivalence between DZ curves and their corresponding VES curves (Zohdy, 1974a). Furthermore, the value of $K$ is always greater than or equal to 1 for all values of $s_i$ in the range $-1 \leq s_i \leq 1$, which makes it suitable for comparison with the values of the deviations

$$\delta_i(I) = \rho_m/\rho_{m_c}. \tag{51}$$

Thus, for each set of points on the $T=f(S)$ line which are fitted by the method of least squares, an intercept with the previous straight line is determined, and the values of $T$ and $S$ at the intersections are used to define the coordinates of $\rho_m{}^* = \rho_1{}^*$, $L_m{}^* = h_1{}^*$, from the equations

$$\rho_m{}^* = \sqrt{T^*/S^*} = \rho_1{}^*,$$

$$L_m{}^* = \sqrt{T^*S^*} = h_1{}^*,$$

and $\rho_2{}^*$ is calculated from the slope of the second straight line $T^* = f(S^*)$.

The values of $\rho_{m_c}$ are calculated successively from equations 37 at the abscissas, $L_m$, for all the averaged DZ points, and if upon the inclusion of the $(I+1)$ point, the deviation $\delta_i(I)$ for $1 \leq i \leq I+1$ is greater than the calculated value of $K_i$ or smaller than $1/K_i$, the $(I+1)$ point is dropped.

The above procedure is successively applied to evaluate the coordinates $(L_m{}^*, \rho_m{}^*)$ of all the fundamental DZ points on the $n$-layer DZ curve. Then, the inversion equations 13 and 14 are used to determine the layer thicknesses and resistivities of the reduced model. The VES

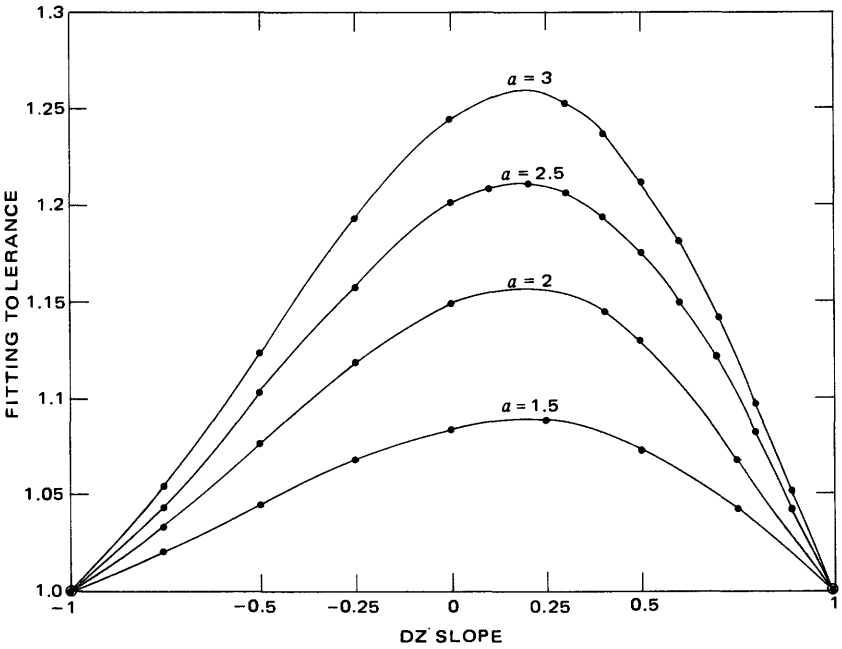


FIGURE 11. — Graph showing the variation of the fitting tolerance, $K$, as a function of the slope of a point on a DZ curve. Values of $a$ in equation 15 are shown on each curve.

curve for the reduced model is calculated to ascertain the equivalence between the calculated and observed models. In the computer program the maximum number of layers in the reduced model is set equal to 10. Thus, if upon the completion of the smoothing process the resulting number of layers is larger than 10, then the constant $a$ in the fitting-tolerance function $K$ is increased from 2 to 4, and, if necessary, to 8, and the smoothing process is repeated.

## FIELD EXAMPLE

Figure 12 shows an example of the results obtained from the automatic interpretation of a deep vertical electrical sounding, VES 19, obtained by Zohdy and Stanley (1973) on the Snake River plain, Idaho. The observed VES curve at the top of the figure was measured with the Schlumberger array to electrode spacings of $AB/2$ = 12,000 feet (≈3,657 m) and with the equatorial array to a maximum spacing of about 68,000 feet (≈20,726 m). The various segments on the curve were shifted downward to conform to the equatorial segment (adjusted curve), and the minor cusps, caused by the crossing of the current electrodes over lateral heterogeneities, were removed to form the smoothed curve.

As shown in the lower part of the figure, the smoothed curve was

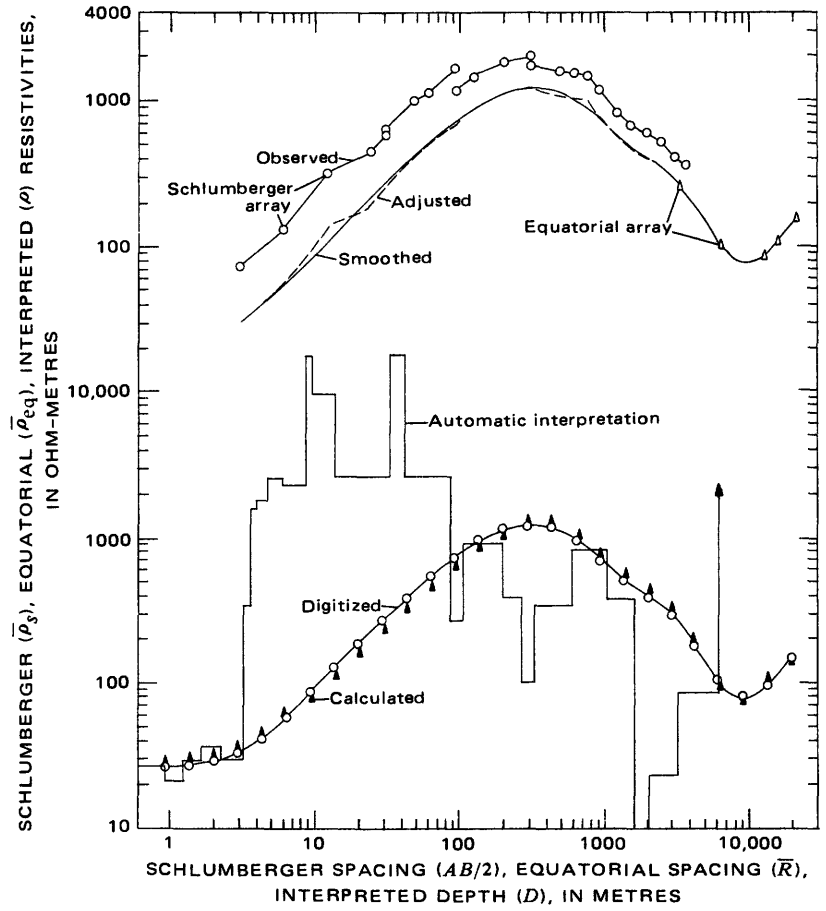


FIGURE 12. — Results of the automatic interpretation of a deep vertical electrical sounding (VES 19) curve obtained on the Snake River Plain, Idaho.

digitized at a logarithmically equal interval, $\Delta$, which corresponds to the rate of 6 points per logarithmic cycle ($\Delta = e^{\ln 10/6}$) to facilitate the use of the Ghosh convolution coefficients (Ghosh, 1971b). The data (which consist of the smallest and largest electrode spacings ($AB/2$) and the values of apparent resistivities at the prescribed digitizing interval) were fed into the computer which performed the automatic interpretation and fitted the digitized curve with the calculated VES curve, as shown in the lower part of the figure. The detailed solution (27 layers corresponding to 27 points on the digitized curve) is also depicted on the lower part of the figure.

There are basically five electrical units on the detailed model, as evidenced by the five major breaks in the distribution of resistivity with

depth. The first unit, with an average resistivity of about 30 ohm-metres, corresponds to a windblown-soil layer. The second unit, with an average resistivity of about 4,000 ohm-metres, represents dry basalts of the Snake River Group. The third unit, at a depth of about 300–400 feet (91.44–121.9 m), is characterized by an average resistivity of about 300–400 ohm-metres and is interpreted as basalt saturated with fresh water. The fourth layer is characterized by low resistivities which range from about 10 ohm-metres to about 100 ohm-metres; most likely these resistivities represent sedimentary rocks, which are possibly intercalated with ash-flow tuffs, and which extend to a depth of about 20,000 feet (6,096 m). The fifth electrical unit is the electric basement, which has a high resistivity (≥1,000 ohm-metres) and may represent Paleozoic rocks of very large thicknesses.

The number of layers in the detailed solution can be reduced either automatically (as explained earlier) or manually by plotting the DZ curve for the 27 layers, smoothing it, and inverting it. Figure 13 shows the 27-layer DZ curve as the dashed curve. A five-layer solution (equations 13 and 14) was obtained by manually selecting the coordinates of the DZ points (1, 2, 5, and 6) designated by the open circles and a six-layer solution was obtained by manually selecting the coordinates of the

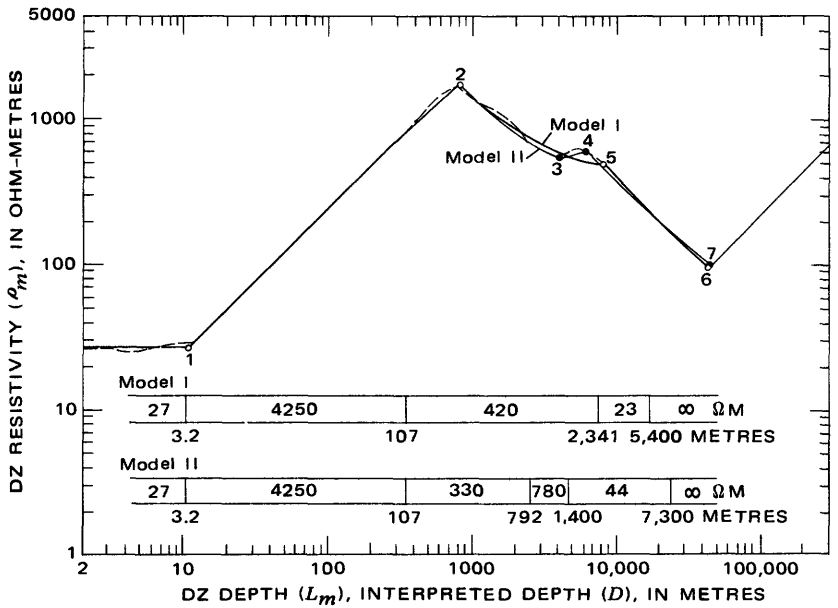


FIGURE 13. — Graph showing two equivalent-layering models obtained by manually smoothing the DZ curve of the detailed solution (dashed curve) and inverting the smoothed DZ curves. Model I is based on the inversion of the DZ points 1, 2, 5, and 6. Model II is based on the inversion of the DZ points 1, 2, 3, 4, and 7.

first two open-circle points (points 1 and 2) and the following three solid-circle points (points 3, 4, and 7). Other equivalent models can be found by automatically or manually smoothing the DZ curve in different ways.

## ADVANTAGES AND LIMITATIONS OF THE METHOD

The advantages of the method of automatic interpretation presented in this paper are:

1. The average processing time for a VES curve covering three logarithmic cycles is about 8 seconds on an IBM 360/65 computer. This makes the method very suitable for the processing of large numbers of VES curves at considerable savings in time and expenditure.
2. Only the values of the smallest and largest electrode spacings, and the ordinates of the apparent resistivities (which must have been digitized at the logarithmic interval of 1.46 along the abscissa) are entered into the computer.
3. The method does not rely on the extension of the left and right branches of the VES curve to their appropriate asymptotes.
4. Distorted field VES curves can be processed and two sets of solutions will result: one based on the inversion of the distorted curve and the other based on the inversion of the automatically smoothed VES curve.
5. The method is extended through the automatic smoothing of DZ curves so that earth models, composed of 10 layers or less, are automatically obtainable.
6. The user does not have to make any preliminary guesses at the number of layers, their thicknesses, or resistivities.
7. The curve-fitting process is made in the VES curve domain rather than in the kernel-function domain. This assures the interpreter of obtaining a valid solution which fits the observed data and is within the possible equivalence for VES curves rather than the wider range of equivalence for TKF curves.

The limitations of the method primarily lie in the limited accuracy of computing VES curves by convolution, using Ghosh's inverse filter coefficients. The calculation of a large variety of VES curves, using Ghosh's nine coefficients indicated the following:

1. The position of the $S$ line will be shifted to the left by about 6 percent if the resistivity of the last layer is assumed to be much greater than about 100 times the overlying layer. This is not a serious problem because, by assuming the resistivity of the last layer to be about 50–100 times the resistivity of the overlying layer, a sufficiently long linear segment on the VES curve will be calculated, and it will coincide with the true $S$ line within about 1 percent.

2. For VES curves with steeply descending branches and for which the ratio of the minimum apparent resistivity, $\bar{\rho}_{s_{min}}$, to the maximum apparent resistivity, $\bar{\rho}_{s_{max}}$, is less than 0.025, the application of Ghosh's coefficients will result in inaccurate apparent resistivity values for values of $\bar{\rho}_{s_{min}}$ which are less than 0.025 $\bar{\rho}_{s_{max}}$. Consequently, the automatic fitting of such curves may be less than satisfactory in the region where $\bar{\rho}_{s_{min}} < 0.025\ \bar{\rho}_{s_{max}}$. For these curves the validity of the solution should be checked by calculating the VES curve for the obtained model using numerical integration methods.

## REFERENCES CITED

Bhattacharya, P. K., and Patra, H. P., 1968, Direct-current geoelectric sounding—Principles and interpretation: New York, Elsevier Publishers, 139 p.

Compagnie Générale de Géophysique, 1963, Master curves for electrical sounding [2d rev. ed.]: The Hague, European Assoc. Explor. Geophysicists.

Crous, C. M., 1971, Computer-assisted interpretation of electrical soundings: Colorado School Mines M.S. Thesis, 108 p.

Flathe, H., 1955, A practical method of calculating geoelectrical model graphs for horizontally stratified media: Geophys. Prosp. [Netherlands], v. 3, no. 3, p. 268–294.

———1963, Five-layer master curves for the hydrogeological interpretation of geoelectric resistivity measurements above a two-storey aquifer: Geophys. Prosp. [Netherlands], v. 11, no. 4, p. 471–508.

Ghosh, D. P., 1971a, The application of linear filter theory to the direct interpretation of geoelectrical resistivity sounding measurements: Geophys. Prosp. [Netherlands], v. 19, no. 2, p. 192–217.

———1971b, Inverse filter coefficients for the computation of apparent resistivity standard curves for a horizontally stratified earth: Geophys. Prosp. [Netherlands], v. 19, no. 4, p. 769–775.

Grove, W. E., 1966, Brief numerical methods, *in* Applied mathematics series: New Jersey, Prentice-Hall, 117 p.

Hildebrand, F. B., 1956, Introduction to numerical analysis: New York, McGraw-Hill Book Co., 511 p.

Kalenov, E. N., 1957, [Interpretation of vertical electrical sounding curves]: Moscow, Gostoptekhizdat, 471 p. [in Russian].

Koefoed, Otto, 1965, Direct methods of interpreting resistivity observations: Geophys. Prosp. [Netherlands], v. 13, no. 4, p. 568–591.

———1966, The direct interpretation of resistivity observations made with a Wenner electrode configuration: Geophys. Prosp. [Netherlands], v. 14, no. 1, p. 71–79.

———1968, The application of the kernel function in interpreting geoelectrical measurements: Geoexploration Mon., ser. 1, no. 2, Stuttgart, Gebrüder Borntraeger, 111 p.

———1970, A fast method for determining the layer distribution from the raised kernel function in geoelectrical sounding: Geophys. Prosp. [Netherlands], v. 18, no. 4, p. 564–570.

Kunetz, Geza, 1966, Principles of direct-current resistivity prospecting: Berlin, Gebrüder Borntraeger, 103 p. [English translation from the French by Robert Van Nostrand].

Kunetz, Geza, and Rocroi, J. P., 1970, Traitement automatique des sondages electriques: Geophys. Prosp. [Netherlands], v. 18, no. 2, p. 157–198.

Maillet, Raymond, 1947, The fundamental equations of electrical prospecting: Geophysics, v. 12, no. 4, p. 529–556.

Meinardus, H. A., 1967, The kernel function in direct-current resistivity sounding: Colorado School Mines D. Sc. Thesis, 151 p.

———1970, Numerical interpretation of resistivity soundings over horizontal beds: Geophys. Prosp. [Netherlands], v. 18, no. 3, p. 415–433.

Mooney, H. M., Orellana, Ernesto, Pickett, Harry, and Tornheim, Leonard, 1966, A resistivity computation method for layered earth models: Geophysics, v. 31, no. 1, p. 192–203.

Onodera, Seibe, 1960, The kernel function in the multiple-layer resistivity problem: Jour. Geophys. Research, v. 65, p. 3787–3794.

Orellana, Ernesto, 1963, Properties and drawing of the so-called Dar Zarrouk curves: Geophysics, v. 28, no. 1, p. 99-110.

Orellana, Ernesto, and Mooney, H. M., 1966, Master tables and curves for vertical electrical sounding over layered structures: Madrid, Interciencia, 150 p., 66 tables.

Pekeris, C. L., 1940, Direct method of interpretation in resistivity prospecting: Geophysics, v. 5, no. 1. p. 31–42.

Rijkswaterstaat, 1969, Standard graphs for resistivity prospecting: The Hague, European Assoc. Explor. Geophysicists.

Schlichter, L. B., 1933, The interpretation of the resistivity prospecting method for horizontal structures: Physics, v. 4, p. 307–322.

Shkabarnia, N. G., and Gritsenko, V. G., 1971, Interpretatsiia kriv'ikh elektricheskogo zondirovaniia s primeneniem EVM: Moscow, Izdatel'ctvo "Nedra," 113 p.

Stefanesco, S. S., Schlumberger, Conrad, and Schlumberger, Marcel, 1930, Sur la distribution électrique potentielle autor d'une prix de terre ponctuelle dans un terrain à couche horizontales, homogenes et isotrope: Jour. Physique et Radium, v. 11, no. 1, p. 132–140.

Strakhov, V. N., 1966a, Numerical methods for the solution of geophysical problems reducing to integral equations with multiplicative kernels [in Russian]: Akad. Nauk SSSR Izv. Ser. Geofiz., 1966, no. 9, p. 38–52; translated by F. Goodspeed, *in* Physics of the Solid Earth, 1966, p. 570–576.

———1966b, The analytic determination of the parameters of a horizontally layered medium from data obtained by vertical electrical prospecting [in Russian]: Akad. Nauk. SSSR Izv. Ser. Geofiz., 1966, no. 4, p. 52–63; translated by F. Goodspeed, *in* Physics of the Solid Earth, 1966 p. 237–242.

———1968, The solution of the inverse problem for vertical electrical sounding [in Russian]: Akad. Nauk. SSSR Izv. Ser. Geofiz., 1968, no. 4, p. 77–84; translated by F. Goodspeed, *in* Physics of the Solid Earth, 1968, p. 247-250.

Strakhov, V. N., and Karelina, G. N., 1969, [On the interpretation of vertical electrical sounding data with an electronic calculating machine]: Prikladnaya Geofizika, v. 56, p. 118-129 [in Russian].

Sunde, E. D., 1949, Earth conduction effects in transmission systems: New York, Van Nostrand, 370 p.

Vanyan, L. L., Morozova, G. M., and Lozhenits'na, L., 1962, [On the calculation of theoretical electrical sounding curves]: Prikladnaya Geofizika, v. 34, p. 135–144 [in Russian].

Vozoff, Keeva, 1958, Numerical resistivity analysis—Horizontal layers: Geophysics, v. 23, no. 3, p. 536–556.

Watson, G. N., 1962, A treatise on the theory of Bessel functions [2d ed.]: Cambridge, Cambridge Univ. Press, 804 p.

Zohdy, A. A. R., 1965, The auxiliary point method of electrical sounding interpretation, and its relationship to the Dar Zarrouk parameters: Geophysics, v. 30, no. 4, p. 644–660.

———1968, The effect of current leakage and electrode spacing errors on resistivity

measurements, *in* Geological Survey research 1968: U.S. Geol. Survey Prof. Paper 600-D, p. D258-D264.

———1974a, Use of Dar Zarrouk curves in the interpretation of vertical electrical sounding data: U.S. Geol. Survey Bull. 1313-D, 41 p.

———1974b, A computer program for the calculation of Schlumberger sounding curves by convolution: available only from U.S. Dept. Commerce Natl. Tech. Inf. Service, Springfield, Va. 22161, as U.S. Geol. Survey Rept. USGS-GD-74-010, PB-232 056.

———1974c, A computer program for the automatic interpretation of Schlumberger sounding curves over horizontally stratified media: available only from U.S. Dept. Commerce Natl. Tech. Inf. Service, Springfield, Va. 22161, as U.S Geol. Survey Rept. USGS-GD-74-017, PB-232 703.

Zohdy, A. A. R., and Jackson, D. B., 1973, Recognition of natural brine by electrical soundings near the Salt Fork of the Brazos River, Kent and Stonewall Counties, Texas: U.S. Geol. Survey Prof. Paper 809-A, 14 p.

Zohdy, A. A. R., and Stanley, W. D., 1973, Preliminary interpretation of electrical sounding curves obtained across the Snake River Plain from Blackfoot to Arco, Idaho: U.S. Geol. Survey open-file report, 5 p.

☆U.S. GOVERNMENT PRINTING OFFICE:1983-381-614/586